Spectral effects of dispersive mode coupling in driven mesoscopic systems

Yaxing Zhang and M. I. Dykman

Spectral effects of dispersive mode coupling in driven mesoscopic systems

Yaxing Zhang[1] and M. I. Dykman[1]

[1]*Department of Physics and Astronomy, Michigan State University, East Lansing, MI 48824, USA*
(Dated: September 28, 2015)

Nanomechanical and other mesoscopic vibrational systems typically have several nonlinearly coupled modes with different frequencies and with long lifetime. We consider the power spectrum of one of these modes. Thermal fluctuations of the modes nonlinearly coupled to it lead to fluctuations of the mode frequency and thus to the broadening of its spectrum. However, the coupling-induced broadening is partly masked by the spectral broadening due to the mode decay. We show that the mode coupling can be identified and characterized using the change of the spectrum by weak resonant driving. We develop a path-integral method of averaging over the non-Gaussian frequency fluctuations from nonresonant (dispersive) mode coupling. The shape of the driving-induced power spectrum depends on the interrelation between the coupling strength and the decay rates of the modes involved, providing a means of characterizing these modes. The analysis is extended to the case of coupling to many modes, which because of the cumulative effect can become effectively strong. We also find the power spectrum of a driven mode where the mode has internal nonlinearity. Unexpectedly, the power spectra induced by the intra- and inter-mode nonlinearities are qualitatively different. The analytical results are in excellent agreement with the numerical simulations.

PACS numbers: 62.25.Fg, 85.25.-j, 78.60.Lc, 05.40.-a

I. INTRODUCTION

Mesoscopic vibrational systems typically have several nonlinearly coupled modes. These can be flexural, torsional, or acoustic modes in the case of nanomechanical resonators[1–8], photon and phonon modes in optomechanics[9–14], or modes of microwave cavities in circuit quantum electrodynamical systems[15]. Often different modes have significantly different frequencies, so that the interaction between them is primarily dispersive. A major effect of such interaction is that the frequency of one mode depends on the amplitude of the other mode. The related shift of the mode frequency provides a means of characterizing the coupling strength where both modes can be accessed, cf. Refs. 3, 7, 16, and 17 and can be used for quantum nondemolition measurements of the oscillator Fock states.[18,19]

In many mesoscopic systems only one or a few modes can be directly accessed and controlled. The presence of dispersive coupling to other modes and the strength of this coupling have to be inferred from the data on the accessible modes. To the best of our knowledge, there have been no generally accepted means of doing this.

An important consequence of dispersive coupling is that amplitude fluctuations of one mode lead to frequency fluctuations of the other mode[20]. The amplitude fluctuations come from the coupling to a thermal reservoir, but they can also be of nonthermal origin. The mode-coupling induced frequency fluctuations broaden the spectrum of the response to an external force and the power spectrum. Such broadening has been suggested as a major broadening mechanism for flexural modes in carbon nanotubes[1], graphene sheets[8], doubly clamped beams[7,16] as well as microcantilevers.[17]

Separating the mode-coupling induced fluctuations from other spectral broadening mechanisms is nontrivial, see Ref. 21 for a recent review of the broadening mechanisms. The most familiar broadening mechanism is vibration decay due to energy dissipation. Another mechanism of interest for the present paper is internal vibration nonlinearity. Because of such nonlinearity, the frequency of a vibrational mode depends on the mode amplitude and thermal fluctuations of the amplitude lead to frequency fluctuations. This is reminiscent of the mode-coupling effect, yet the nonlinearity is different. We show below how the two nonlinearity mechanisms can be clearly distinguished.

In this paper, we propose a means for identifying and characterizing the mode-coupling induced frequency fluctuations. The approach is based on studying the change of the power spectrum of the considered mode, which is due to an additionally applied periodic driving. The approach does not require access to other modes, in contrast to Refs. 3, 7, 16, and 17, for example. It relies on the fact that, quite generally, frequency fluctuations lead to the features in the power spectrum of a periodically driven mode, which do not occur without such fluctuations.[22] If one thinks of the driven mode as a charged oscillator in a stationary radiation field, these features correspond to fluorescence and quasi-elastic light scattering. The absence of these effects in the case of a periodically driven linear oscillator with constant frequency is a textbook result.[23–25]

The analysis of the power spectra of driven modes with fluctuating frequency in Ref. 22 was phenomenological. The results were obtained in several limiting cases and in the case of Gaussian fluctuations. The dispersive mode coupling studied here leads to strongly non-Gaussian frequency fluctuations. The simplest type of such coupling corresponds to the coupling energy $\propto q^2 q_d^2$, where q is the coordinate of the considered driven mode and q_d is the coordinate of the mode to which it is dispersively coupled

and which we call the d-mode. Where the modes are far from resonance, the frequency change of the considered mode is proportional to the period-average value of q_d^2, i.e., to the squared amplitude of $q_d(t)$. Even where $q_d(t)$ is Gaussian, as in the case of thermal displacement of a linear mode,[24] the squared displacement $q_d^2(t)$ is not.

The features of the spectra related to the dispersive-coupling induced frequency fluctuations depend on the interrelation between three parameters. These are the typical magnitude of the frequency fluctuations $\Delta\omega$, their reciprocal correlation time Γ_d, and the decay rate of the considered mode Γ. We assume that all these parameters are small compared to the mode eigenfrequencies and their difference.

In the absence of driving, the power spectrum and the linear response spectrum of the considered mode have the form of a convolution of the spectrum calculated without dispersive coupling and a function that depends on the parameter $\alpha_d = \Delta\omega/\Gamma_d$.[26] We call α_d the motional narrowing parameter to draw the similarity (although somewhat indirect) with the motional narrowing effect in nuclear magnetic resonance (NMR).[27,28] For $\alpha_d \ll 1$ the correlation time of the frequency fluctuations is comparatively small. Then the fluctuations are averaged out and their effect is small, as in the case of fast decay of correlations in NMR. On the other hand, for $\alpha_d \gg 1$, the spectrum can be thought of as a superposition of partial spectra, each for a given value of the amplitude of $q_d(t)$. The weight of the partial spectrum is determined by the probability distribution of this amplitude.

In the presence of driving, the situation is different. The first distinction is that, without the dispersive coupling, there is no driving-induced part of the power spectrum at all, except for the trivial δ-peak at the driving frequency. Based on the previous results,[22] we expect that the driving-induced part of the spectrum will strongly depend on the interrelation between the rates Γ and Γ_d. It is clear that it will also strongly depend on α_d, but this dependence is not known in advance.

The formulation below is in the classical terms. However, as we explain, the results fully apply also to the case where the considered driven mode is quantum, i.e., its energy level spacing is comparable or exceeds the temperature. At the same time, it is essential that the d-mode is classical. The case of the deeply quantum regime of the d-mode is in a way simpler. In this case, the power spectrum of the considered mode without driving can have a pronounced fine structure, with different lines corresponding to different occupation numbers of the d-mode.[20] This is similar to the spectrum of a two-level system dispersively coupled to a quantum vibrational mode[29,30], where the fine structure has been seen in the experiment.[31]

A. The structure of the paper

An important part of the paper is the averaging over the fluctuations of the d-mode. This is an interesting theoretical problem, with direct relevance to the experiment. It involves an explicit calculation of the appropriate path integral. The calculation is presented in Secs. IV and V. These sections as well as Sec. III A can be skipped if one is interested primarily in the predictions for the experiment. Below in Sec. II we give a general expression for the power spectrum of a mode driven by an external field, which applies where the field is comparatively weak, so that the internal nonlinearity of the mode remains small. The effect of the field is most pronounced where it is close to resonance. In Sec. III we derive equations of motion for weakly damped dispersively coupled modes in the rotating wave approximation. Section VI provides the explicit analytical expressions for the driving-induced part of the power spectrum in the limiting cases, which refer to the fast or slow relaxation of the d-mode compared to the relaxation of the driven mode and also to the large or small frequency shift due to the dispersive coupling compared to the relaxation rate of the d-mode. This section also presents results of numerical calculations of the spectra, which are compared with the results of simulations. The last part of the section describes the dependence of the area of the driving-induced peak on the dispersive coupling parameters. Section VII extends the results to dispersive coupling to several modes. In particular, we consider the cumulative effect of dispersive coupling to many, but not too many modes, which may become strong even where the coupling to each of the modes is weak. Section VIII describes the driving-induced part of the power spectrum for a nonlinear oscillator, where the fluctuations of the oscillator frequency are due not to dispersive coupling but to the internal nonlinearity. The last section provides a summary of the results. The transfer-matrix method used to perform the averaging over the dispersive-coupling induced fluctuations and an outline of an alternative derivation of the major result are given in the appendices.

II. DRIVING-INDUCED PART OF THE POWER SPECTRUM

Frequency fluctuations render the mode response to driving random. Generally, the response is nonlinear in the driving strength. Respectively, even for sinusoidal driving, the mode power spectrum $\Phi(\omega)$ is a complicated function of the driving amplitude F and frequency ω_F. The conventional way of measuring the power spectrum of a driven system with coordinate q corresponds to the definition

$$\Phi(\omega) = 2\mathrm{Re} \int_0^\infty dt e^{i\omega t} \langle\langle q(t+t')q(t')\rangle\rangle,$$

where $\langle\langle\cdot\rangle\rangle$ indicates statistical averaging and averaging with respect to t' over the driving period $2\pi/\omega_F$ (sometimes the power spectrum is also defined as $\Phi(\omega)/2\pi$). If the driving is weak, one can keep in $\Phi(\omega)$ only the terms quadratic in F,

$$\Phi(\omega) \approx \Phi_0(\omega) + \frac{\pi}{2}F^2|\chi(\omega_F)|^2\delta(\omega-\omega_F) + F^2\Phi_F(\omega). \quad (1)$$

Here, Φ_0 is the power spectrum in the absence of driving. For the considered underdamped mode, it is a resonant peak at the mode eigenfrequency ω_0, which is due to thermal vibrations; the width of the peak is small compared to ω_0. Function $\chi(\omega)$ is the mode susceptibility, $\Phi_0(\omega) = (2k_BT/\omega_0)\text{Im }\chi(\omega)$ in the classical limit. The term $\propto |\chi(\omega_F)|^2$ describes the contribution of stationary forced vibrations at frequency ω_F.

Of utmost interest to us is the last term in Eq. (1), $\Phi_F(\omega)$. For a linear oscillator with non-fluctuating frequency, this term is equal to zero. Indeed, the motion of such oscillator is a superposition of thermal vibrations and forced vibrations at frequency ω_F, which are uncoupled. Frequency fluctuations affect both thermal vibrations, leading to spectral broadening, and forced vibrations. The latter effect is particularly easy to understand in the case of slow frequency fluctuations. Here, one can think of the amplitude and phase of forced vibrations as being determined by the detuning of the instantaneous mode frequency from the driving frequency. Therefore they fluctuate in time, which leads to the onset of a "pedestal" of the δ-peak at $\omega = \omega_F$ in Eq. (1). Some other limiting cases have been considered earlier.[22].

III. EQUATIONS OF MOTION FOR THE SLOW VARIABLES

We will consider the power spectrum $\Phi(\omega)$ in the case where the mode of interest is dispersively coupled to another mode (mode d). The modes are weakly coupled to a thermal reservoir, so that their decay rates are small. The mode of interest is driven by a periodic field $F\cos\omega_F t$. The Hamiltonian of the system is

$$H = H_0 + H_b + H_i, \qquad H_0 = \frac{1}{2}(p^2 + \omega_0^2 q^2) + \frac{1}{4}\gamma q^4$$
$$+ \frac{1}{2}(p_d^2 + \omega_d^2 q_d^2) + \frac{3}{4}\gamma_d q^2 q_d^2 - qF\cos\omega_F t. \quad (2)$$

Here, p and p_d are the momenta of the considered mode and the d-mode, respectively, ω_0 and ω_d are the mode eigenfrequencies, γ is the parameter of the intrinsic nonlinearity of the considered mode, and γ_d is the dispersive coupling parameter. We do not incorporate the intrinsic nonlinearity of the d-mode, as it will not affect the results if it is small, see below.

The term H_b is the Hamiltonian of the thermal bath (each mode can have its own bath, but we assume that in this case the baths have the same temperature), whereas H_i describes the mode-to-bath coupling. We assume the

coupling to be linear in the modes coordinates, $H_i = qh + q_d h_d$, where h and h_d are functions of the dynamical variables of the bath. Such coupling is the dominant mechanism of relaxation for small mode displacements and velocities. For H_i of this form, the decay rate of the considered mode is[32,33]

$$\Gamma \equiv \Gamma(\omega_0) = \hbar^{-2}\text{Re}\int_0^\infty dt\langle[h^{(0)}(t), h^{(0)}(0)]\rangle e^{i\omega_0 t}, \quad (3)$$

where $h^{(0)}$ is function h calculated in the neglect of the mode-bath coupling. The expression for the decay rate Γ_d of the d-mode is similar to Eq. (3), with $h^{(0)}$ replaced with $h_d^{(0)}$ and ω_0 replaced with ω_d. Parameters Γ, Γ_d correspond to friction coefficients in the phenomenological description of the mode dynamics

$$\ddot{q} + \partial_q H_0 = -2\Gamma\dot{q} - h^{(0)}(t). \quad (4)$$

The analysis below refers to slowly varying amplitudes and phases of the modes and applies even where the above phenomenological description does not apply.[20,32,33]

In what follows we assume that the modes are underdamped, the nonlinearity is weak, and the driving frequency is close to resonance,

$$\Gamma, \Gamma_d, \frac{|\gamma|\langle q^2\rangle}{\omega_0}, \frac{|\gamma_d|\langle q_d^2\rangle}{\omega_0}, |\omega_0 - \omega_F| \ll \omega_0, \omega_d, |\omega_0 - \omega_d|. \quad (5)$$

The condition on γ, γ_d means that the change of the mode frequencies due to the nonlinearity is small compared to the eigenfrequency. However, it does not mean that the effect of the nonlinearity is small, as the frequency change has to be compared with the frequency uncertainty due to the decay Γ, Γ_d. We assume that the nonlinear change of the d-mode frequency, which comes from the dispersive coupling and the internal nonlinearity of the d-mode, is also small compared to ω_d.

A. Stochastic equations for slow variables

Where conditions (5) apply, the motion of the underdamped modes presents almost sinusoidal vibrations with slowly varying amplitudes and phases. It can be described by the standard method of averaging, which is similar to the rotating wave approximation in quantum optics. To this end, we change to complex variables

$$u(t) = \frac{1}{2}[q(t) + (i\omega_F)^{-1}\dot{q}(t)]\exp(-i\omega_F t) \quad (6)$$

and similarly $u_d(t) = \frac{1}{2}[q_d(t) + (i\omega_d)^{-1}\dot{q}_d(t)]\exp(-i\omega_d t)$. Disregarding fast oscillating terms in the equation for $u(t)$, we obtain

$$\dot{u} = -[\Gamma + i\delta\omega_F - i\xi(t)]u - i\frac{F}{4\omega_0} + f(t),$$

$$\delta\omega_F = \omega_F - \omega_0, \quad \xi(t) = \frac{3\gamma}{2\omega_0}|u(t)|^2 + \frac{3\gamma_d}{2\omega_0}|u_d(t)|^2, \quad (7)$$

where $f(t) = -(2i\omega_0)^{-1}h^{(0)}(t)\exp(-i\omega_F t)$. Similarly, the equation for $u_d(t)$ reads

$$\dot{u}_d = -\left[\Gamma_d - i\frac{3\gamma_d}{2\omega_d}|u(t)|^2\right]u_d + f_d(t), \qquad (8)$$

with $f_d(t) = -(2i\omega_d)^{-1}h_d^{(0)}(t)\exp(-i\omega_d t)$.

Functions f, f_d describe the forces on the modes from the thermal bath. The forces are random, and one can always choose $\langle f \rangle = \langle f_d \rangle = 0$. Asymptotically, they are delta-correlated Gaussian noises,

$$\langle f(t)f^*(t')\rangle = (\Gamma k_B T/\omega_0^2)\delta(t-t'),$$
$$\langle f_d(t)f_d^*(t')\rangle = (\Gamma_d k_B T/\omega_d^2)\delta(t-t'); \qquad (9)$$

all other correlators vanish. The δ-functions here are δ-functions in "slow" time compared to $\omega_0^{-1}, \omega_d^{-1}$, and the correlation time of the thermal bath. The stochastic differential equations (7) and (8) are understood in the Stratonovich sense: $\langle u(t)f^*(t)\rangle = \Gamma k_B T/2\omega_0^2$, $\langle u_d(t)f_d^*(t)\rangle = \Gamma_d k_B T/2\omega_d^2$. These equations were obtained and their range of applicability established for a harmonic oscillator coupled to a bath,[32,33] but they also hold for a weakly anharmonic oscillator.[20]

As seen from the definition of the complex amplitude $u(t)$, function $\xi(t)$ in Eq. (7) describes a change of the frequency of the considered mode due to the intrinsic nonlinearity and the dispersive coupling. Because of the noise terms f, f_d, the frequency becomes a random function of time. The related frequency noise is of primary interest for this paper.

IV. THE DRIVING-INDUCED SPECTRUM $\Phi_F(\omega)$ FOR DISPERSIVE COUPLING

In this and the two following sections we will study the spectrum $\Phi_F(\omega)$ in the case where the internal nonlinearity of the mode can be disregarded, i.e., one can set $\gamma = 0$. In this case frequency fluctuations $\xi(t) \propto |u_d(t)|^2$ in Eq. (7) are due only to the dispersive nonlinear mode coupling. An important feature of this coupling is that it does not affect the frequency noise $\xi(t)$ itself, as essentially was noticed earlier.[26] In other words, fluctuations of $|u_d(t)|^2$ are the same as if the d-mode were just a linear oscillator uncoupled from the considered mode.

The simplest way to see this is to change in the equation of motion (8) from $u_d(t)$ to $\tilde{u}_d(t) = K(t)u_d(t)$ with $K(t) = \exp[-3i(\gamma_d/2\omega_d)\int^t dt'|u(t')|^2]$. The Langevin equation for $\tilde{u}_d$ is $\dot{\tilde{u}}_d = -\Gamma_d\tilde{u}_d + \tilde{f}_d(t)$ with $\tilde{f}_d(t) = K(t)f_d(t)$. From Eq. (9), the noise $\tilde{f}_d(t)$ has the same correlation functions as $f_d(t)$. Therefore the term $\propto \gamma_d$ drops out of the equation for $\tilde{u}_d$. Since $|u_d|^2 = |\tilde{u}_d|^2$, the term $\propto \gamma_d$ does not affect $|u_d(t)|^2$ either [even though it does affect $u_d(t)$].

It is convenient to write $\xi(t)$ in terms of the scaled real and imaginary part of $\tilde{u}_d = (2\omega_0/3|\gamma_d|)^{1/2}(Q_d + iP_d)$. Functions Q_d, P_d are the scaled quadratures of a damped

harmonic oscillator. They are described by the independent exponentially correlated Gaussian noises (the Ornstein-Uhlenbeck noises)[34]. Using the Langevin equation for $\tilde{u}_d$, we obtain

$$\langle Q_d(t)Q_d(0)\rangle = \langle P_d(t)P_d(0)\rangle = \alpha_d\Gamma_d\exp(-\Gamma_d|t|),$$
$$\alpha_d = 3|\gamma_d|k_B T/8\omega_0\omega_d^2\Gamma_d,$$
$$\xi(t) = [Q_d^2(t) + P_d^2(t)]\text{sgn}\gamma_d. \qquad (10)$$

The frequency noise of the driven mode $\xi(t)$ is non-Gaussian. Parameter α_d characterizes the ratio of the standard deviation of the noise, which is equal to the noise mean value $\langle\xi(t)\rangle = 3\gamma_d k_B T/4\omega_0\omega_d^2$, to its correlation rate Γ_d.

Since $\xi(t)$ is independent of $u(t)$, the Langevin equation for $u(t)$ (7) is linear. Its solution reads

$$u(t) = \int_{-\infty}^t dt'\chi_{\text{sl}}^*(t,t')[(-iF/4\omega_0) + f(t')],$$
$$\chi_{\text{sl}}(t,t') = e^{-(\Gamma-i\delta\omega_F)(t-t')}\exp\left[-i\int_{t'}^t dt''\xi(t'')\right]. \qquad (11)$$

Function $\chi_{\text{sl}}(t,t')$ describes the response of the considered driven mode to a resonant perturbation. The coefficient at F averaged over realizations of $\xi(t)$ gives the resonant susceptibility of the mode,

$$\chi(\omega_F) = \frac{i}{2\omega_0}\int_0^\infty dt\langle\chi_{\text{sl}}(t,0)\rangle. \qquad (12)$$

It determines the δ-peak in the power spectrum (1). From Eq. (11), the term $\Phi_F(\omega)$ in Eq. (1) for the power spectrum has the form

$$\Phi_F(\omega) = (8\omega_0^2)^{-1}\text{Re}\int_0^\infty dt\exp[i(\omega-\omega_F)t]$$
$$\times\left[\int_{-\infty}^t dt'\int_{-\infty}^0 dt_1'\langle\chi_{\text{sl}}(t,t')\chi_{\text{sl}}^*(0,t_1')\rangle - 4\omega_0^2|\chi(\omega_F)|^2\right] \qquad (13)$$

(in the integral over t it is implied that Im $\omega \to +0$).

The term $\propto f(t')$ in Eq. (11) determines the power spectrum of the mode $\Phi_0(\omega)$ near its maximum, $|\omega - \omega_0| \ll \omega_0$, in the absence of driving. Thus, Eqs. (11) - (13) give a general expression for the power spectrum of an underdamped mode with fluctuating frequency in the absence of internal nonlinearity.

V. AVERAGING OVER THE FREQUENCY NOISE FOR DISPERSIVE COUPLING

To find the driving-induced part of the power spectrum $F^2\Phi_F(\omega)$, one has to perform averaging over fluctuations of $\xi(t)$ in Eq. (13). This calculation is the central theoretical part of the paper. In what follows we outline the critical steps that are involved.

The integrand in the expression for $\Phi_F(\omega)$ can be written as

$$\langle \chi_{\text{sl}}(t,t')\chi_{\text{sl}}^*(0,t_1')\rangle = e^{-(\Gamma-i\delta\omega_F)(t-t')+(\Gamma+i\delta\omega_F)t_1'}$$
$$\times G^2(t,t',t_1'), \quad G^2(t,t',t_1') = \langle e^{-i\phi_\xi(t,t')+i\phi_\xi(0,t_1')}\rangle,$$
$$\phi_\xi(t,t') = \int_{t'}^t dt''\xi(t''). \tag{14}$$

Here, $\phi_\xi(t,t')$ is the increment of the phase of the oscillator over the time interval (t',t) due to the frequency noise $\xi(t)$. Function G describes the result of the averaging over the noise.

Expression (14) can be slightly simplified using the relation (10) between $\xi(t)$ and the quadratures Q_d and P_d. These quadratures are statistically independent, and therefore averaging over them can be done independently, so that

$$G(t,t',t_1') = \left\langle \exp\left[i\int_{t_0}^t dt'' k(t'')Q_d^2(t'')\right]\right\rangle, \tag{15}$$

where $t_0 = \min(t',t_1')$ and in the interval $t_0 < t'' < t$ function $k(t'')$ is equal to $0,\pm 1$,

$$k(t'') = \begin{cases} -\text{sgn}\gamma_d, & \tau \le t'' \le t; \quad \tau = \max(t',0) \\ 0, & \tau' < t'' < \tau; \quad \tau' = \max\left(\min(0,t'),t_1'\right) \\ \text{sgn}(t'-t_1')\text{sgn}\gamma_d, & t_0 = \min(t',t_1') \le t'' \le \tau'. \end{cases} \tag{16}$$

The averaging in Eq. (15) can be conveniently done using the path-integral technique. A theory of the power spectrum based on this technique was previously developed for the case where there is no driving.[26] The approach[26] can be extended to the present problem, as

discussed in the Appendix B. However, the calculation is cumbersome. Here we use a different method, which is based on the technique[35] for calculating determinants in path integrals.

In terms of a path integral, the mean value of a functional $L[Q_d(t)]$ of $Q_d(t)$ can be written as $\int \mathcal{D}Q_d(t)L[Q_d(t)]\mathcal{P}[Q_d(t)]$. For the considered exponentially correlated noise $Q_d(t)$, the probability density functional is (cf. Ref. 36)

$$\mathcal{P}[Q_d(t)] = \exp\left[-(4\alpha_d\Gamma_d^2)^{-1}\int dt(\dot{Q}_d + \Gamma_d Q_d)^2\right].$$

To find $G(t,t',t_1')$ we need to perform averaging over the values of $Q_d(t'')$ in the interval (t_0,t). In a standard way, we discretize the time as $t_n = t_0 + n\epsilon, n = 0,\ldots,N$, where $\epsilon = (t-t_0)/N$ and $N \gg 1$. The path integral is then reduced to integrating over the values of $Q_n \equiv Q_d(t_n)/(4\alpha_d\Gamma_d^2\epsilon)^{1/2}$ with $1 \le n \le N$ followed by averaging over $Q_0 \equiv Q_d(t_0)/(4\alpha_d\Gamma_d^2\epsilon)^{1/2}$ with the Boltzmann weighting factor $\exp[-2\epsilon\Gamma_d Q_0^2]$.

In the mid-point discretization, in the integrals over time one uses $\dot{Q}(t) \to [Q(t) - Q(t-\epsilon)]/\epsilon$ and $f(Q(t)) \to [f(Q(t)) + f(Q(t-\epsilon))]/2$ for an arbitrary $f(Q)$.[37] Then the exponent in $\mathcal{P}[Q(t)]$ becomes

$$-(4\alpha_d\Gamma_d^2)^{-1}\int dt(\dot{Q}+\Gamma_d Q)^2 \to -\sum_{n=1}^N\left[(Q_n-Q_{n-1})^2\right.$$
$$+\epsilon^2\Gamma_d^2 Q_n^2\right] - \epsilon\Gamma_d(Q_N^2 - Q_0^2). \tag{17}$$

The integral over t'' in Eq. (15) is similarly discretized and goes over into $4\alpha_d\Gamma_d^2\epsilon^2\sum_n k_n Q_n^2$ with $k_n \equiv k(t_n)$. Then the expression for function G becomes

$$G(t,t',t_1') = I[k]/I[0], \qquad I[k] = \int dQ_0 e^{-Q_0^2(1+\epsilon\Gamma_d)}\int\prod_{n=1}^N dQ_n \exp\left[-\mathbf{Q}^\dagger\hat{\Lambda}[k]\mathbf{Q} + 2Q_0 Q_1\right]. \tag{18}$$

Here, $\mathbf{Q}$ is a vector with components $Q_1,\ldots,Q_N$. From Eq. (17), the diagonal matrix elements of $\hat{\Lambda}[k]$ are $\Lambda_{nn}[k] = 2 + \epsilon^2\Gamma_d^2(1 - 4i\alpha_d k_n)$ for $1 \le n \le N-1$, $\Lambda_{NN}[k] = 1 + \epsilon^2\Gamma_d^2(1-4i\alpha_d k_N)+\epsilon\Gamma_d$. The only non-zero off-diagonal matrix elements of $\hat{\Lambda}$ are $\Lambda_{n\,n\pm 1}[k] = -1$.

A. Finding the determinant

The integrals in Eq. (18) are Gaussian. Therefore the calculation of G requires finding the determinants of the matrices $\hat{\Lambda}[k]$ and $\hat{\Lambda}[0]$. This can be done following the approach[35]. We consider the determinant $D_n \equiv D_n[k]$ of the square submatrix of $\hat{\Lambda}[k]$, which is located at the

lower right corner and has rank $N - n + 1$. For example, D_1 is the determinant of the whole matrix $\hat{\Lambda}$, whereas D_N is the matrix element Λ_{NN}. The result of integration over $Q_1,\ldots,Q_N$ in Eq. (18) for $I[k]$, besides the Q_0-dependent factor discussed below, is $\pi^{N/2}/\sqrt{D_1[k]}$.

It is straightforward to see that D_n satisfies the recurrence relation

$$D_n = [2+\epsilon^2\Gamma_d^2(1-4i\alpha_d k_n)]D_{n+1}-D_{n+2}, \quad 1 \le n \le N-2. \tag{19}$$

In the limit $\epsilon \to 0$, $D_n[k]$ goes over into $D(t_n;k)$ and Eq. (19) reduces to a differential equation for $D(t'') \equiv D(t'';k)$,

$$\ddot{D}(t'') - \Gamma_d^2[1 - 4i\alpha_d k(t'')]D(t'') = 0 \tag{20}$$

The obvious boundary conditions for function D are $D(t) = \lim_{\epsilon \to 0} D_N = 1$ and $\dot{D}(t) = \lim_{\epsilon \to 0}(D_N - D_{N-1})/\epsilon = -\Gamma_d$. The quantity of interest is $D_1[k] \approx D(t_0; k)$; we will also need $\dot{D}(t_0; k)$, see below.

The integration of the linear in Q_1 term in the exponent in Eq. (18) gives the factor $\exp[Q_0^2(\hat{\Lambda}^{-1})_{11}]$. It follows from the above analysis that $(\hat{\Lambda}^{-1})_{11} = D(t_0 + 2\epsilon)/D(t_0 + \epsilon) \approx 1 + \epsilon \dot{D}(t_0)/D(t_0)$. Then the result of integration over Q_0 in Eq. (18) is the factor $\{\pi/\epsilon[\Gamma_d - \dot{D}(t_0; k)/D(t_0; k)]\}^{1/2}$ in $I[k]$.

For $k = 0$, we have from Eq. (20) $D(t''; 0) = \exp[\Gamma_d(t - t'')]$. With this, the expression (18) for function G becomes

$$G(t, t', t_1') = \left\{ 2\Gamma_d e^{\Gamma_d(t-t_0)}/[\Gamma_d D(t_0; k) - \dot{D}(t_0; k)] \right\}^{1/2} \tag{21}$$

This expression is the central result of the section. It reduces the problem of calculating the driving-induced part of the power spectrum to solving an ordinary differential equation (20).

B. The average susceptibility

We start the discussion of the applications of the general result (21) with the analysis of the factor $\langle \chi_{\rm sl}(t, 0) \rangle$, which gives the average mode susceptibility, Eq. (12). Function $\langle \chi_{\rm sl}(t, 0) \rangle$ is given by $\langle \exp[-i \int_0^t dt'' \xi(t'')] \rangle$, which in turn is given by Eq. (14) with G of the form of Eq. (15) in which $t' = t_1' = 0$ and $k(t'') = -\text{sgn}\gamma_d$. Solving Eq. (20) with $k(t'') = \text{const}$ is straightforward, as is also finding then $G(t, 0, 0)$ from Eq. (21). The result reads

$$\langle \chi_{\rm sl}(t, 0) \rangle = \exp\left[-(\Gamma - i\delta\omega_F)t\right] \tilde{\chi}(t), \qquad \tilde{\chi}(t) = e^{\Gamma_d t}$$
$$\times \left[\cosh a_d t + (\Gamma_d/a_d)(1 + 2i\alpha_d \text{sgn}\gamma_d) \sinh a_d t\right]^{-1},$$
$$a_d = \Gamma_d(1 + 4i\alpha_d \text{sgn}\gamma_d)^{1/2}. \tag{22}$$

Equation (22) expresses the average susceptibility in elementary functions. It agrees with the result[26] for the correlation function of the mode dispersively coupled to a fluctuating mode.

C. The average of the product of the susceptibilities

Solving the full Eq. (20) with discontinuous $k(t'')$ is more complicated. It can be done by finding function $D(t'')$ piecewise where $k(t'') = \text{const}$ as a sum of "incident" and "reflected" waves and then matching the solutions. The corresponding method reminds the transfer matrix method. It is described in Appendix A. The result

reads

$$[G(t, t', t_1')]^{-2} = [\tilde{\chi}(\tau_1)\tilde{\chi}'(\tau_3)]^{-1} - \frac{(\Gamma_d^2 - a_d^2)(\Gamma_d^2 - a_d'^2)}{4\Gamma_d^2 a_d a_d'}$$
$$\times \sinh(a_d \tau_1) \sinh(a_d' \tau_3) \exp[-\Gamma_d(2\tau_2 + \tau_1 + \tau_3)] \tag{23}$$

where $\tau_1 = t - \tau, \tau_2 = \tau - \tau', \tau_3 = \tau' - t_0$; parameters t_0, τ, and τ' are expressed in terms of t, t', t_1' in Eq. (16), and $\tilde{\chi}(t)$ is given by Eq. (22). Function $\tilde{\chi}'(t) = \tilde{\chi}(t)$ and $a_d' = a_d$ for $t' < t_1'$, whereas $\tilde{\chi}'(t) = \tilde{\chi}^*(t)$ and $a_d' = a_d^*$ for $t' > t_1'$.

This expression is unexpectedly simple. We use it below for analytical calculations, in particular for calculating the driving-induced part of the power spectrum in the limiting cases.

VI. DISCUSSION OF RESULTS

In this section we use the above results to discuss the form of the driving-induced part $F^2 \Phi_F(\omega)$ of the power spectrum in the case of dispersive coupling. We give explicit expressions for the spectrum in the limiting cases. We also present the results of the numerical calculations of the spectrum based on the general expressions (13), (14), and (23). These results are compared with the simulations. The simulations were performed in a standard way by integrating the stochastic equations of motion (7) - (9) using the Heun scheme[38].

As we show, the shape and the magnitude of $\Phi_F(\omega)$ sensitively depend on two factors. One is the interrelation between the magnitude of frequency fluctuations $\Delta\omega$ and their bandwidth $2\Gamma_d$, the motional-narrowing parameter α_d defined in Eq. (10). The other is the interrelation between Γ_d and the width of the mode spectrum in the absence of driving $\Phi_0(\omega)$.

The width of the mode spectrum is not given just by the mode decay rate Γ. It is affected by the frequency noise and depends on α_d. This is seen from Eqs. (12) and (22) for the susceptibility Im $\chi(\omega)$, cf. Ref. 26. The halfwidth of the peak of Im $\chi(\omega)$ varies with the frequency noise strength $\alpha_d \Gamma_d$ from $\Gamma + 2\alpha_d^2 \Gamma_d$, for $\alpha_d \ll 1$, to $\sim \Gamma + 2\alpha_d \Gamma_d$ for $\alpha_d \gg 1$ (the peak of Im $\chi(\omega)$ is profoundly non-Lorentzian for $\alpha_d \gg 1$ and $\alpha_d \Gamma_d \gtrsim \Gamma$).

An important outcome of the analysis in the previous sections is that the spectrum $\Phi_F(\omega)$ allows one to measure both the strength and the correlation time of the frequency noise due to dispersive coupling. In the first place, it allows one to directly identify the very presence of this noise. We emphasize that the full driving-induced term in the power spectrum $F^2 \Phi_F(\omega)$ can be seen even where thermal fluctuations of the driven mode are weak and the peak in the power spectrum $\Phi_0(\omega)$ is too small to be resolved.

A. The spectrum $\Phi_F(\omega)$ in the limiting cases

1. Weak frequency noise

The general expression for the spectrum simplifies in the limiting cases where the frequency noise is weak or its bandwidth is large or small compared to the width of the driven mode spectrum $\Phi_0(\omega)$. In the case of dispersive coupling, the limit of weak frequency noise is realized where $\alpha_d \Gamma_d \ll \Gamma$. A general expression for $\Phi_F(\omega)$ for weak frequency noise was obtained earlier[22]. It relates $\Phi_F(\omega)$ to the power spectrum of the frequency noise $\xi(t)$. From Eq. (10), in the present case we have $\langle \xi(t) \rangle = 2\langle Q_d^2(t) \rangle \mathrm{sgn}\,\gamma_d = 2\alpha_d \Gamma_d \mathrm{sgn}\,\gamma_d$, whereas the correlation function of the noise deviation from the average $\delta\xi(t) = \xi(t) - \langle \xi(t) \rangle$ is $4\alpha_d^2 \Gamma_d^2 \exp(-2\Gamma_d|t|)$. Then, extending the results[22] to noise with non-zero average, we obtain

$$\Phi_F(\omega) = (\alpha_d^2 \Gamma_d^3 / \omega_0^2)[(\omega_F - \tilde{\omega}_0)^2 + \Gamma^2]^{-1}$$
$$\times \{[(\omega - \omega_F)^2 + 4\Gamma_d^2][(\omega - \tilde{\omega}_0)^2 + \Gamma^2]\}^{-1}, \qquad (24)$$

where $\tilde{\omega}_0 = \omega_0 + \langle \xi(t) \rangle = \omega_0 + 2\alpha_d \Gamma_d \mathrm{sgn}\gamma_d$. This expression can be also directly obtained from Eq. (23) in the corresponding limit.

From Eq. (24), for weak dispersive-coupling induced noise, the intensity of the spectrum $\Phi_F(\omega)$ is proportional to the square of the coupling parameter. If the detuning of the driving field frequency from the eigenfrequency of the driven oscillator largely exceeds the half widths of the power spectra of the both oscillators in the absence of driving, $|\omega_F - \tilde{\omega}_0| \gg \Gamma, \Gamma_d$, the power spectrum $\Phi_F(\omega)$ has two distinct peaks. One is located at the oscillator frequency $\tilde{\omega}_0$ and has halfwidth Γ. The other is located at the driving frequency ω_F and has halfwidth $2\Gamma_d$. We note that the noise variance $4\alpha_d^2 \Gamma_d^2$ is independent of Γ_d. For constant $\alpha_d^2 \Gamma_d^2$, the areas of the peaks at $\tilde{\omega}_0$ and ω_F are $\propto \Gamma_d/\Gamma\delta\omega_F^4$ and $\delta\omega_F^{-4}$, respectively (the ratio Γ_d/Γ affects only the area of the peak at ω_0). As $|\delta\omega_F|$ decreases, the peaks start overlapping. For small $|\delta\omega_F|$ they cannot be resolved. This behavior is general and occurs also where the frequency noise is not weak, as we show below.

2. Broad-band frequency noise

We now consider the case of the broad-band frequency noise, where the decay rate of the d-mode Γ_d largely exceeds the width of the driven mode spectrum. This condition requires that the motional-narrowing parameter be small, $\alpha_d \ll 1$. At the same time, the contribution of the frequency noise to the spectrum width of the considered mode does not have to be small compared to its decay rate, i.e., the ratio $\alpha_d^2 \Gamma_d/\Gamma$ can be arbitrary. In other words, the broadening of the spectrum of the considered mode can still largely come from the dispersive coupling.

To describe the most pronounced peak in the spectrum $\Phi_F(\omega)$ for large Γ_d and small α_d, one can solve Eq. (20) in the WKB approximation, $D(t'') \approx \exp\{-\Gamma_d \int_t^{t''} dt_2[1 - 4i\alpha_d k(t_2)]^{1/2}\}$. Combined with Eq. (21), this solution immediately gives the averaging factor G in Eq. (14) and thus the spectrum Φ_F. Alternatively, one can use the explicit expression (23) for function G. Only the first term has to be kept in this expression for $\alpha_d \ll 1$ and $\Gamma \ll \Gamma_d$. Integration over time in Eq. (13) gives

$$\Phi_F(\omega) \approx \frac{2\alpha_d^2 \Gamma_d/\Gamma}{4\omega_0[\tilde{\Gamma}^2 + (\omega_F - \tilde{\omega}_0)^2]} \mathrm{Im}\,\chi(\omega),$$
$$\chi(\omega) = (i/2\omega_0)[\tilde{\Gamma} - i(\omega - \tilde{\omega}_0)]^{-1}. \qquad (25)$$

Parameters $\tilde{\Gamma}$ and $\tilde{\omega}_0$ are the halfwidth of the spectrum and the eigenfrequency of the driven mode renormalized due to the dispersive coupling, $\tilde{\Gamma} = \Gamma + 2\alpha_d^2 \Gamma_d$ and $\tilde{\omega}_0$ is the same as in Eq. (24).

Equation (25) shows that, for a broad-band frequency noise, the spectrum $\Phi_F(\omega)$ has the same shape as the spectrum in the absence of driving, $\Phi_F(\omega) \propto \Phi_0(\omega) \propto \mathrm{Im}\,\chi(\omega)$. However, from the spectrum $\Phi_0(\omega)$, which is Lorentzian in this case, one cannot tell whether the spectrum halfwidth $\tilde{\Gamma}$ is due to decay or to frequency fluctuations. In contrast, $\Phi_F \propto \alpha_d^2$ is proportional to the variance of the frequency noise and has a characteristic temperature dependence ($\alpha_d^2 \propto T^2$ if Γ_d is T-independent). It enables identifying the frequency noise contribution to the spectral broadening, as it was earlier demonstrated for a δ-correlated frequency noise.[22]

Along with the comparatively narrow peak (25), for $\alpha_d^2 \Gamma_d \gtrsim \Gamma$ the spectrum $\Phi_F(\omega)$ has a broad background near ω_0, with the typical frequency scale Γ_d. To describe it one has to take into account corrections $\propto \alpha_d^2$ to the leading-order term in function G (23). For large $|\delta\omega_F| \gg \tilde{\Gamma}$, the spectrum also has a peak near ω_F with width $\sim 2\Gamma_d$.

3. Narrow-band frequency noise

The spectrum $\Phi_F(\omega)$ has a characteristic shape also in the opposite limit where the bandwidth of the frequency noise $2\Gamma_d$ is small compared to the width of the spectrum in the absence of driving $\Phi_0(\omega)$. In this case $\Phi_F(\omega)$ displays a characteristic peak at the driving frequency ω_F, as can be already inferred from the weak-noise expression (24). In the overall spectrum $\Phi(\omega)$ it looks like a pedestal of the δ-peak at ω_F. The typical halfwidth of the pedestal is given by Γ_d. This allows one to read off the decay rate of the d-mode from the spectrum $\Phi_F(\omega)$ without accessing the d-mode directly. To resolve the pedestal for large α_d, where $\alpha_d \Gamma_d \gtrsim \Gamma$ so that the width of the spectrum $\Phi_0(\omega)$ is primarily determined by the dispersive coupling, we need a comparatively large detuning of the driving frequency from the maximum of $\Phi_0(\omega)$.

The simplest way to find $\Phi_F(\omega)$ near ω_F for small Γ_d is based on Eq. (23). One first notices from Eq. (13) that the major contribution to $\Phi_F(\omega)$ in this case comes from

the time range $t \sim \Gamma_d^{-1}$, whereas $t-t', |t_1'| \lesssim |\Gamma - i\delta\omega_F|^{-1}$. Therefore in Eq. (23) one is interested in the limit of large t but comparatively small $t - t', |t_1'|$. In the limit $t \rightarrow \infty$ but for fixed $t - t'$, function $G^{-2}(t, t', t_1') \rightarrow 1/\tilde{\chi}(t - t')\tilde{\chi}^*(-t_1')$ with $\tilde{\chi}(t)$ given by Eq. (22). The remaining term in G^{-2} is $\propto \exp(-2\Gamma_d t)$. One can then write the integrand in the expression (13) for $\Phi_F(\omega)$ as a series in $\exp(-2\Gamma_d t)$. The next simplification comes from the fact that $|a_d(t - t')|, |a_d t_1'| \ll 1$ for $|\Gamma - i\delta\omega_F|/|a_d| \gg 1$. Therefore one can expand $\tilde{\chi}(t - t') \approx [1 + 2i\alpha_d\Gamma_d(t - t')]^{-1}$ and similarly for $\tilde{\chi}^*(-t_1')$. Ultimately, the result of integration over the times t, t', t_1' reads

$$\Phi_F(\omega) = \sum_{n=1}^{\infty} \left| \frac{1}{n!} \alpha_d^n \frac{\partial^n}{\partial \alpha_d^n} \chi(\omega_F) \right|^2 \frac{n\Gamma_d}{(\omega - \omega_F)^2 + (2n\Gamma_d)^2}. \quad (26)$$

This expression describes the spectral peak at small $|\omega - \omega_F|$ in terms of the derivatives of the susceptibility $\chi(\omega)$ calculated as a function of the motional-narrowing parameter α_d. The width of the spectral peak (26) is given by the bandwidth of the frequency noise $2\Gamma_d$. The peak is generally non-Lorentzian.

B. Evolution of $\Phi_F(\omega)$ with the varying bandwidth and strength of the frequency noise

To visualize the dependence of the spectrum $\Phi_F(\omega)$ on the parameters of the system, we now present the results of numerical evaluation of the general expressions (13), (14), and (23). Fig. 1 shows the evolution of the driving-induced power spectrum $\Phi_F(\omega)$ with the varying ratio of the decay rates Γ_d/Γ, i.e., the varying ratio of the bandwidth of the frequency noise and the decay rate of the driven mode. We use as a scaling factor the susceptibility χ_0 of the driven mode in the absence of dispersive coupling,

$$\chi_0(\omega_F) = i[2\omega_0(\Gamma - i\delta\omega_F)]^{-1}. \quad (27)$$

In Fig. 1 (a), the frequency noise bandwidth is much larger than the width of the spectrum $\Phi_0(\omega)$ in the absence of driving. The spectrum $\Phi_F(\omega)$ is close to a Lorentzian centered near the shifted eigenfrequency of the driven mode, see Eq. (25); for small α_d the shift should be $2\alpha_d\Gamma_d$, whereas the halfwidth should be close to $\Gamma + 2\alpha_d^2\Gamma_d$,[26] which agrees with the numerics. In Fig. 1 (d), on the other hand, the noise bandwidth is small. The spectrum $\Phi_F(\omega)$ is a narrow peak near the driving frequency ω_F, see Eq. (26), with halfwidth $\approx \Gamma_d$. In Figs. 1 (b) and (c) the frequency noise bandwidth is comparable to the width of the spectrum $\Phi_0(\omega)$. In this case the spectrum $\Phi_F(\omega)$ displays two partly overlapping peaks. The overlapping can be reduced by tuning the driving frequency ω_F further away from the resonance, see below.

Fig. 2 shows the evolution of the spectrum $\Phi_F(\omega)$ with the varying strength (standard deviation) $2\alpha_d\Gamma_d$ of the

frequency noise. The frequency noise bandwidth $2\Gamma_d$ is chosen to be close to the decay rate of the driven mode Γ. The driving frequency ω_F is tuned away from resonance so that the two peaks of $\Phi_F(\omega)$ are well separated. An insight into the shape of the peaks can be gained from the aforementioned similarity of the spectrum $\Phi_F(\omega)$ with the spectrum of fluorescence and quasi-elastic light scattering by a periodically driven oscillating charge.

For weak frequency noise, curve 1 in Fig. 2 , the peaks are located near ω_F (quasi-elastic scattering) and ω_0 (fluorescence), cf. Eq. (24). As the noise strength increases, the peak near ω_0 becomes broader and the position of its maximum shifts to higher frequency (if $\gamma_d > 0$, as assumed in the figure). This resembles the evolution of the spectrum $\Phi_0(\omega)$ in the absence of driving with increasing α_d; this evolution is shown in the inset of Fig. 2. For $\alpha_d > 1$ the peak becomes non-Lorentzian and asymmetric.

In contrast, the shape of the peak located near ω_F stays almost the same with varying noise strength. This is consistent with the picture of quasi-elastic scattering, where the width of the peak is determined by the frequency noise bandwidth. To illustrate how persistent this behavior is, we scaled the spectra in Fig. 2 so that at their maxima at ω_F the spectra have the same height for different α_d.

C. Effect on $\Phi_F(\omega)$ of the detuning of the driving frequency

To provide more insight into the nature of the double-peak structure of the spectrum $\Phi_F(\omega)$ for $\Gamma \sim \Gamma_d$, we show in Fig. 3 the effect of detuning of the driving frequency ω_F from resonance. Panels (a), (b), and (c) refer to the driving frequency being red detuned, equal to, and blue detuned from the the maximum of the spectrum $\Phi_0(\omega)$ in the absence of driving, respectively. The results we show refer to the dispersive coupling constant $\gamma_d > 0$. For $\gamma_d < 0$, the plots should be mirror-reflected with respect to $\omega - \omega_0$, and $\omega_F - \omega_0$ should be replaced with $\omega_0 - \omega_F$.

The peak located near the frequency ω_F is well resolved in Fig. 3 (a). It moves along with ω_F as the latter varies. In Fig. 3 (a) one can also see a broader peak, which is located close to ω_0 and essentially does not change its position as ω_F changes. For small frequency-noise bandwidth, the peak at ω_F becomes narrow and is described by Eq. (26). However, it is well-resolved for large frequency detuning even where the noise bandwidth and the width of the spectrum $\Phi_0(\omega)$ are of the same order of magnitude. If the widths are close and ω_F is close to resonance, the peaks overlap and cannot be identified, as seen in panel (b). The areas of the peaks are dramatically different for red and blue detuning. This is due to the asymmetry of the spectrum $\Phi_0(\omega)$ in the presence of the frequency noise induced by dispersive coupling, see the inset of Fig. (2). As seen from Fig. 1, for very small
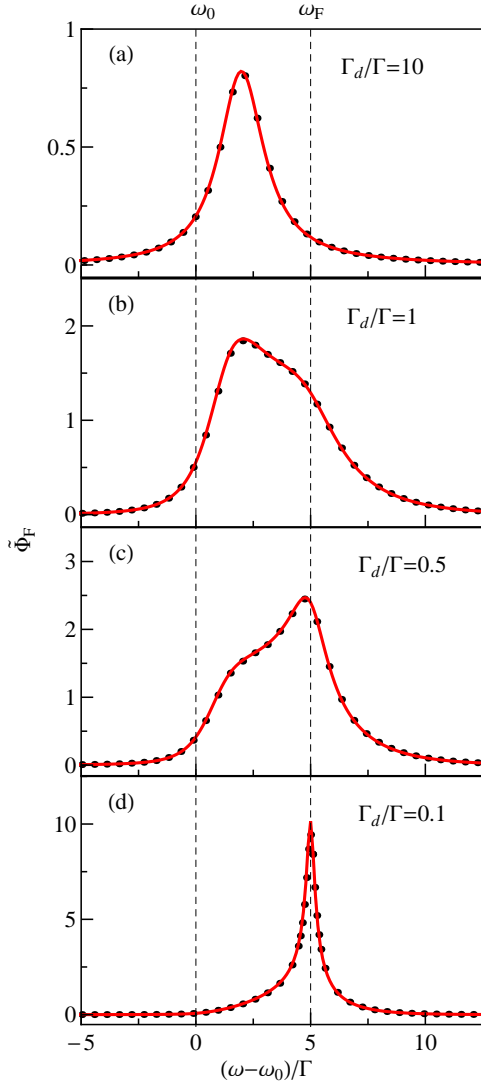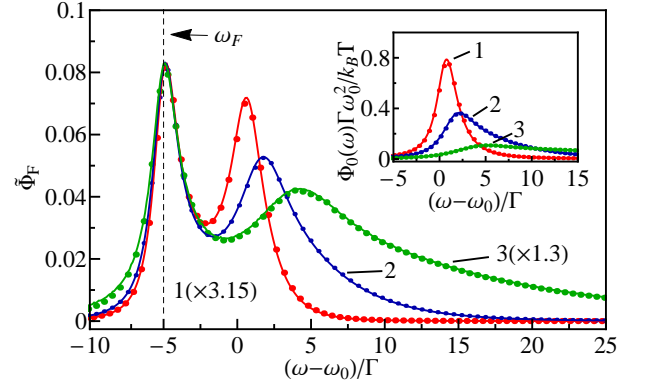
FIG. 2. The evolution of the driving-induced part of the power spectrum with the varying strength of the frequency noise due to dispersive coupling. Curve 1 to 3 refer to the scaled standard deviation of the noise $\alpha_d \Gamma_d/\Gamma = 0.5$, 2.5, and 12.5, respectively. The ratio of the noise bandwidth to the decay rate of the driven mode is $2\Gamma_d/\Gamma = 1$. The scaled detuning of the driving frequency from the eigenfrequency of the driven mode is $\delta\omega_F/\Gamma = -5$. The spectrum is scaled using the noise-free susceptibility $\chi_0(\omega_F)$, Eq. (27), $\tilde{\Phi}_F = 4\Gamma\Phi_F/|\chi_0(\omega_F)|^2$. The curves 1 and 3 are additionally scaled by factors 3.15 and 1.3, respectively, so that the peaks near ω_F have the same height. The inset shows the spectrum $\Phi_0(\omega)$ in the absence of driving for the same values of the frequency noise strength $\alpha_d \Gamma_d/\Gamma$ as in the main panel. The solid lines and the dots show the analytical theory and the simulations, respectively.

FIG. 1. The scaled driving-induced part of the power spectrum of the driven mode dispersively coupled to another mode, which we call the d-mode. Thermal fluctuations of the d-mode lead to frequency fluctuations of the driven mode. Panels (a) to (d) show the change of the spectrum with the varying ratio Γ_d/Γ of the decay rates of the d-mode and the driven mode. The scaled strength (standard deviation) of the frequency noise is $\alpha_d \Gamma_d/\Gamma = 1$. The spectrum $\Phi_F(\omega)$ is scaled using the noise-free susceptibility $\chi_0(\omega_F)$, Eq. (27), $\tilde{\Phi}_F = 4\Gamma\Phi_F/|\chi_0(\omega_F)|^2$. The solid lines and the dots show the analytical theory and the numerical simulations, respectively.

Γ_d/Γ the peak near the oscillator eigenfrequency disappears; this was discussed earlier in the case of weak noise, but is also true in a general case.

D.   The area of the driving induced power spectrum

The area S_F of the driving induced power spectrum $\Phi_F(\omega)$ is defined as $S_F = \int_0^\infty d\omega \Phi_F(\omega)$. The major con-

tribution to the integral comes from the frequency range where $|\omega - \omega_F|, |\omega - \omega_0| \ll \omega_F$. Then integration over ω in Eq. (13) gives a factor $2\pi\delta(t)$. Further simplification comes from changing from integrating over t' and t'_1 to integrating over t' and $t' - t'_1$ and using Eq. (12) for the susceptibility of the mode. The result reads

$$S_F = \frac{\pi}{4\omega_0\Gamma}\mathrm{Im}\chi(\omega_F) - \frac{\pi}{2}|\chi(\omega_F)|^2. \qquad (28)$$

This reduces the calculation of the area S_F just to finding the susceptibility $\chi(\omega_F)$ of the mode. This susceptibility with account taken of the dispersive coupling is given by Eqs. (12) and (22).

The behavior of the area S_F can be found explicitly for small and large α_d. In the limit of small α_d, where the frequency noise is weak, from Eq. (24) $S_F \propto \alpha_d^2$. For large α_d, it is convenient to write $\tilde{\chi}(t)$ in Eq. (22) as $\tilde{\chi}(t) \approx (2/\sqrt{i\alpha_d}) \sum_{n=0}^\infty \exp[-2n(i\alpha_d)^{-1/2} - (2n+1)a_dt]$, where we assumed $\gamma_d > 0$; the ultimate result is independent of the sign of γ_d. The susceptibility $\chi(\omega_F)$ is given by the integral of $\tilde{\chi}(t)$ over t, Eq. (12). In the limit $\Gamma_d\alpha_d^{1/2} \gg |\Gamma - i\delta\omega_F|$ from Eq. (12) $\chi(\omega_F) \approx (2\omega_0\alpha_d\Gamma_d)^{-1} \sum \exp[-2n(i\alpha_d)^{-1/2}]/(2n+1)$. To the leading order in $1/\alpha_d$ this gives

$$\chi(\omega_F) \approx \left[\frac{1}{2}\ln(4\alpha_d) + i\frac{\pi}{4}\right]/4\omega_0\Gamma_d\alpha_d. \qquad (29)$$

We see from Eqs. (28) and (29) that $S_F \propto \alpha_d^{-1}$ falls down
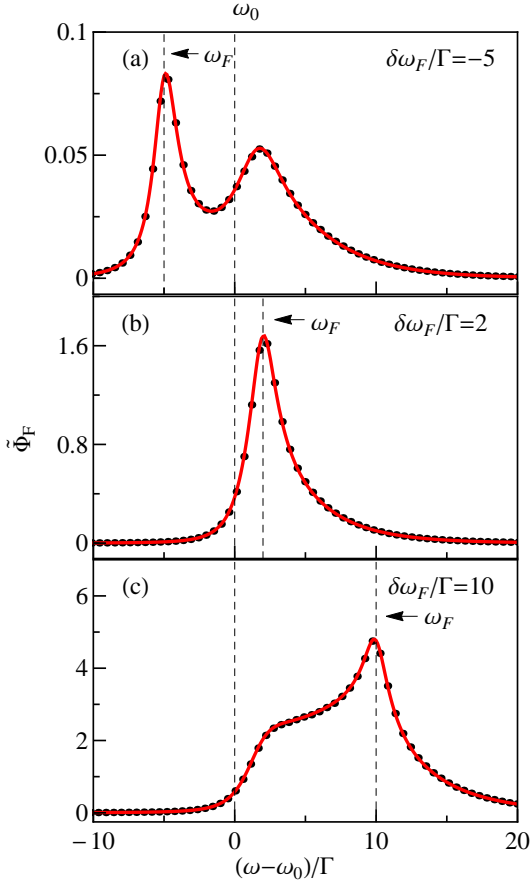
seen in Fig. 4 (b).

FIG. 3. The evolution of the driving-induced part of the power spectrum with the varying detuning of the driving frequency ω_F. The scaled strength of the frequency noise induced by the dispersive coupling is $\alpha_d \Gamma_d / \Gamma = 2.5$. The ratio of the noise bandwidth to the decay rate of the driven mode is $2\Gamma_d / \Gamma = 1$. The spectrum is scaled using the noise-free susceptibility $\chi_0(\omega_F)$, Eq. (27), $\tilde{\Phi}_F = 4\Gamma \Phi_F / |\chi_0(\omega_F)|^2$. The solid lines and the dots show the analytical theory and the simulations, respectively.
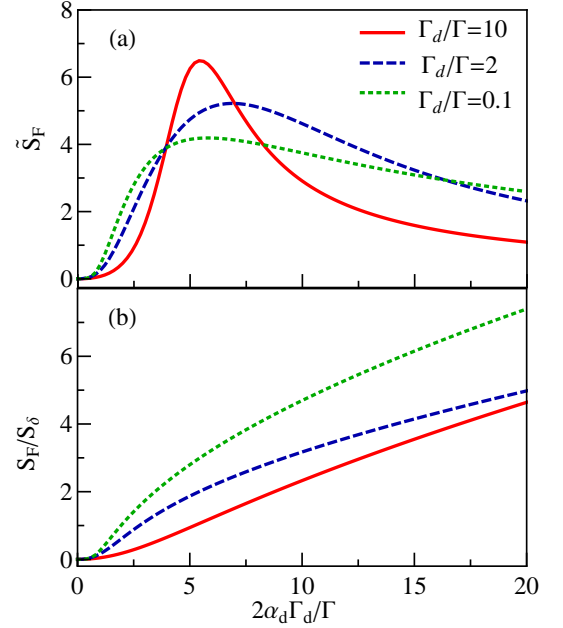

FIG. 4. The area of the driving-induced part of the power spectrum as a function of α_d for different ratio of the frequency noise bandwidth to the decay rate of the driven mode $2\Gamma_d / \Gamma$. The red (solid), blue (dashed), and green (dotted) lines refer to $\Gamma_d / \Gamma = 10$, 2, and 0.1, respectively. The relative detuning of the driving frequency is $\delta\omega_F / \Gamma = 5$. In panel (a), the area S_F is scaled using the noise-free susceptibility $\chi_0(\omega_F)$, Eq. (27), $\tilde{S}_F = 2S_F / \pi |\chi_0(\omega_F)|^2$. In panel (b), S_F is scaled by the area of the δ peak in the power spectrum of the driven mode, $S_\delta = \pi |\chi(\omega_F)|^2 / 2$.

with increasing α_d for large α_d.

The nonmonotonic dependence of the area S_F on the parameter α_d, which is expected from the above asymptotic expressions, is indeed seen in Fig. 4(a). This figure shows the area S_F as a function of the motional narrowing parameter α_d for different Γ_d / Γ. The position of the maximum of S_F sensitively depends on Γ_d / Γ.

In terms of a comparison with experiment, it is advantageous to scale the spectrum Φ_F, and in particular the area S_F, by the area of the δ-peak in the power spectrum of the driven mode. This area is given by the expression $S_\delta = (\pi/2)|\chi(\omega_F)|^2$, cf. Eq. (1). The quantities measured in the experiment are $F^2 S_F$ and $F^2 S_\delta$. The unknown scaled field intensity F^2 drops out from their ratio. From Eqs. (28) and (29) $S_F / S_\delta \propto \alpha_d / \ln^2 \alpha_d$ increases with α_d for large α_d. For small α_d, $S_F / S_\delta \propto \alpha_d^2$ also increases with α_d. On the whole, we found that S_F / S_δ monotonically increases with α_d. This increase is

VII. DISPERSIVE COUPLING TO SEVERAL MODES

The results can be easily extended to the case of dispersive coupling to several modes rather than a single d-mode. We enumerate the modes by the subscript $\varkappa = 1, 2, \ldots$. The modes eigenfrequencies and decay rates are $\omega_\varkappa$ and $\Gamma_\varkappa$. The energy of the dispersive coupling is $(3/4) \sum_\varkappa \gamma_\varkappa q^2 q_\varkappa^2$. The contributions of different modes $\varkappa$ to the frequency fluctuations of the studied mode and therefore to the random accumulation of its phase are additive and mutually independent. To describe the driving-induced spectrum, one can use Eqs. (13) and (14) and average over the phase accumulation in Eq. (14) independently for each mode $\varkappa$. The result is the product of the averages [functions $G(t, t', t'_1)$] calculated for each mode taken separately.

Perhaps of utmost physical interest are the cases where of significance is either dispersive coupling to one or very few modes, as for example in some optomechanical systems in which a radiation mode is dispersively coupled to a mechanical mode[9,19], or where there is dispersive

coupling to many modes, as may be the case in carbon nanotubes or graphene membranes[1,8]. The present paper is focused on the first case. The second case may be simpler, since the parameters $\gamma_\varkappa$ of coupling to individual modes are small; in particular, in nanomechanical systems this is a consequence of the difference of the spatial structure of the studied mode and the modes $\varkappa$. If the number of the $\varkappa$-modes is N, in the thermodynamic limit, $N \to \infty$, we would have $\gamma_\varkappa \propto 1/N$. In this limit the spectrum of the modes $\varkappa$ is almost continuous, and frequency fluctuations of the studied mode come from the coupling $\propto \sum_{\varkappa,\varkappa'} \gamma_{\varkappa\varkappa'} q^2 q_\varkappa q_{\varkappa'}$. This coupling leads to quasielastic scattering of modes $\varkappa$ off the studied mode, which results in a broad-band frequency noise and in the Lorentzian spectrum $\Phi_0(\omega)$;[39,40] the spectrum $\Phi_F(\omega)$ for a broad-band frequency noise is discussed in Ref. 22.

A. An intermediate number of modes: weak and effectively strong coupling

A more interesting situation can arise in the intermediate case of a large but limited number N of modes $\varkappa$. We assume that the mode frequencies are well separated, $|\omega_\varkappa - \omega_{\varkappa'}| \gg \Gamma_\varkappa, \Gamma_{\varkappa'}$, and the frequency differences do not resonate with $\omega_0, 2\omega_0$. Because N is large, the motional-narrowing parameters $\alpha_\varkappa = 3|\gamma_\varkappa| k_B T / 8\omega_0 \omega_\varkappa^2 \Gamma_\varkappa$ are small, $\alpha_\varkappa \ll 1$. However, $\alpha_\varkappa$ are not infinitesimally small. For a large N, one can think of a situation where the cumulative effect of the coupling to many modes is effectively strong.

For a multimode coupling, the factor $\tilde{\chi}(t)$ in the average susceptibility $\langle \chi_{sl}(t,0) \rangle$ (22) is given by the product of the expressions (22) for $\tilde{\chi}(t)$ calculated for each mode $\varkappa$.[26] For $\alpha_\varkappa \ll 1$

$$\tilde{\chi}(t) \approx \exp \sum_\varkappa g_\varkappa(t), \qquad g_\varkappa(t) = -2i\alpha_\varkappa \Gamma_\varkappa t \, \mathrm{sgn}\gamma_\varkappa$$
$$+ \alpha_\varkappa^2 \left[1 - 2\Gamma_\varkappa t - \exp(-2\Gamma_\varkappa t) \right]. \tag{30}$$

For large N, the most simple relevant case is the case of weak coupling, where $\sum_\varkappa \alpha_\varkappa^2 \ll 1$. In this case the power spectrum $\Phi_0(\omega) = (2k_B T/\omega_0)\mathrm{Im}\,\chi(\omega)$ is close to Lorentzian. From Eqs. (12), (22), and (30), to the leading order in $\sum_\varkappa \alpha_\varkappa^2$,

$$\mathrm{Im}\,\chi(\omega) \approx \tilde{\Gamma} / \left\{ 2\omega_0 [\tilde{\Gamma}^2 + (\omega - \tilde{\omega}_0)^2] \right\},$$
$$\tilde{\omega}_0 = \omega_0 + 2\sum_\varkappa \alpha_\varkappa \Gamma_\varkappa \mathrm{sgn}\gamma_\varkappa, \quad \tilde{\Gamma} = \Gamma + 2\sum_\varkappa \alpha_\varkappa^2 \Gamma_\varkappa. \tag{31}$$

In contrast to the previous work,[26] we do not assume here that the halfwidth of the spectrum is close to Γ; even for small $\alpha_\varkappa$ the dispersive-coupling induced spectral broadening may become comparable to the decay rate of the studied mode for $\Gamma_\varkappa \gg \Gamma$. For $\tilde{\Gamma} - \Gamma \ll \Gamma$ one should keep in $\mathrm{Im}\,\chi(\omega)$ other corrections $\propto \alpha_\varkappa^2$, which make the spectrum slightly non-Lorentzian.[26]

Even where $\alpha_\varkappa \ll 1$, the sum $\sum_\varkappa \alpha_\varkappa^2$ is not necessarily small. We will now consider the case where $\sum_\varkappa \alpha_\varkappa^2 \Gamma_\varkappa^2$ greatly exceeds the squared decay rates of the involved modes $\Gamma_\varkappa^2$ (typically, this requires that $\sum_\varkappa \alpha_\varkappa^2 \gg 1$) and $\sum_\varkappa \alpha_\varkappa^2 \Gamma_\varkappa^2 \gg \Gamma^2$. This is the case of cumulatively strong coupling, where the coupling becomes strong because of the large number of modes involved. One can see that the major contribution to the Fourier transform of $\tilde{\chi}(t)$ in Eq. (30), which gives the susceptibility $\chi(\omega)$, comes from the time range $t \lesssim (\sum_\varkappa \alpha_\varkappa^2 \Gamma_\varkappa^2)^{-1/2} \ll \Gamma_\varkappa^{-1}$. Therefore the exponent in Eq. (30) can be expanded to second order in $\Gamma_\varkappa t$. Then the power spectrum in the absence of driving $\Phi_0(\omega) = (2k_B T/\omega_0)\mathrm{Im}\,\chi(\omega)$ has a Gaussian spectral peak. From Eqs. (12), (22), and (30),

$$\mathrm{Im}\,\chi(\omega) \approx (\pi/8\omega_0^2\sigma^2)^{1/2} \exp[-(\omega - \tilde{\omega}_0)^2 / 2\sigma^2],$$
$$\sigma^2 = 4\sum_\varkappa \alpha_\varkappa^2 \Gamma_\varkappa^2. \tag{32}$$

A Gaussian shape of the spectrum in the case of multimode dispersive coupling was proposed to describe the spectra of vibrational modes in carbon nanotubes.[1] This shape was justified[1] in numerical simulations of a model where all $\Gamma_\varkappa$ were the same. The numerical analysis[1] further showed that the tails of the spectrum are Lorentzian, which is generic for nonlinearly coupled modes[26] and is seen from Eq. (30).

1. The driving-induced spectrum

The spectrum $\Phi_F(\omega)$ is determined by the Fourier transform of function $G^2(t, t', t_1')$ which, as indicated earlier, is given by the product of expressions (23) calculated for each mode $\varkappa$. For small $\alpha_\varkappa$

$$G^2(t, t', t_1') \approx \exp\big[g_\varkappa(\tau_1) + g_\varkappa'(\tau_3) + \mathrm{sgn}(t' - t_1')$$
$$\times \sum_\varkappa \alpha_\varkappa^2 e^{-2\Gamma_\varkappa\tau_2} \left(1 - e^{-2\Gamma_\varkappa\tau_1}\right)\left(1 - e^{-2\Gamma_\varkappa\tau_3}\right)\big], \tag{33}$$

where $g_\varkappa$ is given by Eq. (30), whereas $g_\varkappa' = g_\varkappa$ for $t' < t_1'$ and $g_\varkappa' = g_\varkappa^*$ for $t' > t_1'$; the relation between $\tau_{1,2,3}$ and t, t', t_1' is explained below Eq. (23), see also Appendix C.

For small $\sum_\varkappa \alpha_\varkappa^2$ and small frequency-noise induced spectral broadening, $\sum_\varkappa \alpha_\varkappa^2 \Gamma_\varkappa \ll \Gamma$ and $\sum_\varkappa \alpha_\varkappa^2 \Gamma_\varkappa^2 \ll \Gamma^2$, the driving-induced spectrum is given by Eq. (24) in which the factor $\alpha_d^2 \Gamma_d^3 / [(\omega - \omega_F)^2 + 4\Gamma_d^2]$ is replaced by $\sum_\varkappa \alpha_\varkappa^2 \Gamma_\varkappa^3 / [(\omega - \omega_F)^2 + 4\Gamma_\varkappa^2]$ and $\tilde{\omega}_0$ is given by Eq. (31). In the case where $\sum_\varkappa \alpha_\varkappa^2 \Gamma_\varkappa \gtrsim \Gamma$, the spectrum $\Phi_F(\omega)$ has a narrow peak near $\tilde{\omega}_0$ described by Eq. (25) in which one should use Eq. (31) for $\tilde{\Gamma}, \tilde{\omega}_0$, and $\chi(\omega)$, and should replace in the numerator $\alpha_d^2\Gamma_d$ with $\sum_\varkappa \alpha_\varkappa^2 \Gamma_\varkappa$.

The driving-induced term $\Phi_F(\omega)$ arises also in the case of the effectively strong coupling where $\sum_\varkappa \alpha_\varkappa^2 \Gamma_\varkappa^2$ largely exceeds the squared decay rates $\Gamma^2, \Gamma_\varkappa^2$. In this case one should keep in the exponent in G^2 in Eq. (33) only terms up to second order in τ_1, τ_3. Function G^2 then should be expanded in a series in $\sum_\varkappa \alpha_\varkappa^2 \Gamma_\varkappa^2 \tau_1 \tau_3 \exp[-2\Gamma_\varkappa \tau_2]$. The

result of the calculation is given in Appendix C. The general expressions simplify in the important case where the decay rate of the considered mode is small compared to the decay rates of the $\varkappa$-modes, $\Gamma \ll \Gamma_\varkappa$. In this case

$$\Phi_F(\omega) \approx (2\Gamma)^{-1}\mathrm{Im}\chi(\omega)\,\mathrm{Im}\chi(\omega_F). \qquad (34)$$

Equations (32) and (34) show that, for frequency noise with the correlation time small compared to the mode lifetime Γ^{-1}, the leading-order term in the driving-induced power spectrum $\Phi_F(\omega)$ has the same shape as the peak in the power spectrum in the absence of driving $\Phi_0(\omega)$. This behavior was found earlier[22] for a general frequency noise provided the noise spectrum is much broader than the width of the spectral peak of $\Phi_0(\omega)$ and the standard deviation of the noise, in which case the spectrum $\Phi_0(\omega)$ is Lorentzian; cf. also Eq. (25). In the present case the coupling is strong and the width of the noise spectrum $\sim \max\Gamma_\varkappa$ is smaller than the standard deviation σ, and as a result $\Phi_F(\omega)$ is not proportional to the squared coupling parameter as in Eq. (25).

Other terms in the expression for $\Phi_F(\omega)$ obtained in Appendix C show that the driving-induced spectrum is nonmonotonic also near the driving frequency. The structure of the spectrum sensitively depends on the coupling and the decay rates of the $\varkappa$-modes.

The general expressions (C1) and (C3) simplify if all $\varkappa$ modes have the same decay rate. In this case it is also possible to simulate the spectra numerically. We have checked that the analytical results are in excellent agreement with the simulations. It is important that the dispersive-coupling induced term in the power spectrum of the driven mode $\Phi_F(\omega)$ is always positive, whether the dispersive coupling is mostly to one mode or to many modes.

VIII. POWER SPECTRUM OF A DRIVEN NONLINEAR OSCILLATOR

An important contribution to the broadening of the spectra of mesoscopic oscillators can come from their internal nonlinearity.[41] The vibration frequency of a nonlinear oscillator depends on the vibration amplitude. Therefore thermal fluctuations of the amplitude lead to frequency fluctuations. The analysis of the spectra is complicated by the interplay of the frequency fluctuations that come from the amplitude fluctuations and the frequency uncertainty that comes from the oscillator decay. Nevertheless the linear susceptibility could be found for an arbitrary relation between the standard deviation of the frequency $\Delta\omega$ and the decay rate Γ.[26]. The power spectrum of a nonlinear oscillator in the absence of driving is generally asymmetric and non-Lorentzian.

Finding the driving-induced terms in the power spectrum is still more complicated. The oscillator displacement is nonlinear in the driving field amplitude F, and the driving-induced part of the power spectrum $\Phi(\omega)$ is not quadratic in F. However, if the field is weak, Eq. (1)

for $\Phi(\omega)$ applies. In the calculation of $\Phi_F(\omega)$ one should take into account terms in the oscillator displacement that are quadratic in F, which is generic for nonlinear systems.[42]

We assume that the nonlinear part of the oscillator energy is small compared to the linear part. Then the nonlinear term in the oscillator energy can be taken in the form of $\gamma q^4/4$.[43] The oscillator equation of motion in the rotating wave approximation is similar to Eq. (7), except that it now contains the term due to the internal nonlinearity,

$$\dot{u} = -(\Gamma + i\delta\omega_F)u + \frac{3i\gamma}{2\omega_0}|u|^2 u - i\frac{F}{4\omega_0} + f(t). \qquad (35)$$

In this section we do not discuss the effect of dispersive coupling, and the frequency noise that comes from this coupling is not included into Eq. (35).

To find $\Phi_F(\omega)$, we first consider the dynamics of a driven nonlinear oscillator without fluctuations and then take fluctuations into account. The stationary solution u_{st} of Eq. (35) in the absence of the noise $f(t)$ can be found by setting $\dot{u} = 0$. For weak driving, u_{st} is a series in F, which contains only odd powers of F. Since we are interested in the terms which are linear or quadratic in F, it is sufficient to keep only the leading term, $u_{\mathrm{st}} = F/4i\omega_0(\Gamma + i\delta\omega_F)$. One then substitutes into Eq. (35) $u(t) = u_{\mathrm{st}} + \delta u(t)$. The deviation $\delta u(t)$ is due only to the noise,

$$\begin{aligned}\delta\dot{u} = &-(i\delta\omega_F + \Gamma)\delta u + \frac{3i\gamma}{2\omega_0}\left(|\delta u|^2\delta u + 2u_{\mathrm{st}}|\delta u|^2 + u_{\mathrm{st}}^*\delta u^2\right.\\ &\left.+2|u_{\mathrm{st}}|^2\delta u + u_{\mathrm{st}}^2\delta u^*\right) + f(t).\end{aligned} \qquad (36)$$

Time evolution of $\delta u(t)$ depends on the driving field in terms of u_{st}. We find this time evolution in the two limiting cases.

A. Weak nonlinearity

The analysis of the dynamics simplifies in the case of small nonlinearity-induced spread of the oscillator frequency $\Delta\omega$ compared to the decay rate Γ. As seen from Eq. (35), in the absence of driving the frequency shift is quadratic in the vibration amplitude $\propto |u|^2$,[43], and therefore the frequency spread is determine by the standard deviation of $|u|^2$ due to the thermal noise. This gives $\Delta\omega = 3|\gamma|k_B T/8\omega_0^3$.

For $\Delta\omega \ll \Gamma$, it is sufficient to keep only the linear in δu terms in Eq. (36).[44,45] A straightforward calculation then gives a simple expression for the the driving-induced power spectrum,

$$\Phi_F(\omega) \approx \frac{3\gamma k_B T}{8\omega_0^5}\frac{(\omega - \omega_0)\Gamma}{(\Gamma^2 + \delta\omega_F^2)[\Gamma^2 + (\omega - \omega_0)^2]^2}. \qquad (37)$$

The spectrum (37) is proportional to the derivative of the Lorentzian spectrum of the harmonic oscillator

$\Phi_0(\omega) \propto 1/[\Gamma^2 + (\omega - \omega_0)^2]$ over ω. It has a characteristic dispersive shape, being of the opposite signs on the other sides of ω_0. This is the result of the shift of the oscillator vibration frequency $\propto \gamma F^2$ due to the driving. Such shift is the main effect of the driving for small $\Delta\omega/\Gamma$.

B. Large detuning of the driving field frequency

For arbitrary $\Delta\omega/\Gamma$, the analysis is simplified if the detuning of the driving field frequency from the small-amplitude oscillator frequency $|\delta\omega_F| \gg \Gamma, \Delta\omega$. In this case, one can change variables in Eq. (36) to $\delta\tilde{u}(t) = \delta u(t)e^{i\delta\omega_F t}$. The right-hand side of the resulting equation for $\delta\tilde{u}$, besides the noise term, has terms that smoothly depend on time on the scale $|\delta\omega_F|^{-1}$ and terms that oscillate as $\exp(\pm i\delta\omega_F t), \exp(2i\delta\omega_F t)$. These oscillating terms can be considered a perturbation. To the first order of the perturbation theory, the equation for the smooth terms takes the form

$$\delta\dot{\tilde{u}} = -\Gamma\delta\tilde{u} + \frac{3i\gamma}{\omega_0}|u_{\text{st}}|^2\delta\tilde{u}$$
$$+ \left(1 + \frac{9\gamma|u_{\text{st}}|^2}{\omega_0\delta\omega_F}\right)\frac{3i\gamma}{2\omega_0}|\delta\tilde{u}|^2\delta\tilde{u} + \tilde{f}(t), \qquad (38)$$

where $\tilde{f}(t) = f(t)e^{i\delta\omega_F t}$. We keep in this equation the terms $\propto |u_{\text{st}}|^2 \propto F^2$. These terms contribute to the spectrum $\Phi_F(\omega)$. The terms of higher oder in $|u_{\text{st}}|^2$ have been discarded.

Equation (38) has the same form as the equation of motion for the complex amplitude $u(t)$ in the absence of driving, i.e., Eq. (35) with $F = 0$. The noise $\tilde{f}(t)$ has the same correlation function as $f(t)$. Therefore the power spectrum of $\delta\tilde{u}(t)$ is the same as the power spectrum of a nonlinear oscillator found earlier,[26] with the renormalized parameters: the eigenfrequency is shifted by $3\gamma|u_{\text{st}}|^2/\omega_0$ and the nonlinearity parameter is multiplied by the factor $1 + 9\gamma|u_{\text{st}}|^2/\omega_0\delta\omega_F$. We note that the correction $\propto |u_{\text{st}}|^2$ in this factor, which comes from the perturbation theory in $1/\delta\omega_F$, is small.

To find $\Phi_F(\omega)$ we have to expand the result[26] with the appropriately renormalized parameters to the first order in $|u_{\text{st}}|^2$. This gives

$$F^2\Phi_F(\omega) = \beta\{\partial_\beta[\Phi_0(\omega - 2\beta\delta\omega_F; \Delta\omega(1 + 6\beta))]\}_{\beta=0},$$
$$\Phi_0(\omega; \Delta\omega) = \frac{k_BT}{\omega_0^2}\text{Re}\int_0^\infty dt \exp\{[i(\omega - \omega_0) + \Gamma]t\}$$
$$\times [\cosh(at) + (\Gamma/a)(1 + 2i\alpha\text{sgn}\gamma)\sinh(at)]^{-2}. \qquad (39)$$

The parameters α and a have the same structure and the same physical meaning as the parameters α_d and a_d used before, $\alpha = \Delta\omega/\Gamma$ and $a = \Gamma(1 + 4i\alpha\text{sgn}\gamma)^{1/2}$, whereas $\beta = 3\gamma F^2/32\omega_0^3(\delta\omega_F)^3$ is the scaled intensity of the driving field.

The major contribution to $\Phi_F(\omega)$ as given by Eq. (39) for large $|\delta\omega_F|/\Delta\omega$ comes from the frequency shift of the

spectrum without driving $\Phi_0(\omega)$ and is determined by $-2\delta\omega_F\partial_\omega\Phi_0(\omega; \Delta\omega)$. Physically, this results again corresponds to the shift of the oscillator eigenfrequency associated with the forced vibrations, and the spectrum Φ_F again has the characteristic shape of a dispersive curve. To the next order in $1/\delta\omega_F$, the driving broadens or narrows the spectrum depending on the sign of $\gamma/\delta\omega_F$ by renormalizing the nonlinearity-induced standard deviation of the oscillator frequency $\Delta\omega$.
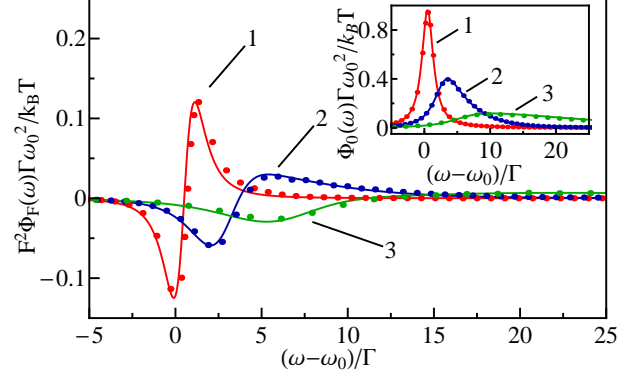

FIG. 5. The driving-induced part of the power spectrum of a nonlinear oscillator for large detuning of the driving frequency, $\delta\omega_F/\Delta\omega = 40$. The solid curves and the dots show the analytical expressions and the results of simulations, respectively. The values of the nonlinearity parameter and the scaled driving strength for the curves 1 to 3 are, respectively, $\alpha \equiv \Delta\omega/\Gamma = 0.125, 1.25$, and 5, and $\beta \equiv 3\gamma F^2/32\omega_0^3\delta\omega_F^3 = 0.016, 0.004$, and 0.004. The inset shows the change of the power spectrum in the absence of driving with varying $\Delta\omega/\Gamma$.

C. Numerical simulations

The analytical results on the spectra of the modulated nonlinear oscillator, Eq. (39), are compared with the results of numerical simulations in Fig. 5. The spectrum $\Phi_F(\omega)$ generally has a positive and negative parts, in a dramatic distinction from the case of a linear oscillator dispersively coupled to another oscillator. As $\Delta\omega/\Gamma$ increases, the shape of $\Phi_F(\omega)$ becomes more complicated, in particular, the positive and negative parts become asymmetric.

The simulations were performed in the same way as for the dispersively coupled modes by integrating the stochastic differential equations (35). We verified that the values of the modulating field amplitude F were in the range where the driving-induced term in the power spectrum was quadratic in F. As seen from this figure, the simulations are in excellent agreement with the analytical results.

In the intermediate range, where the nonlinearity is not weak and the driving is not too far detuned, i.e., $|\delta\omega_F| \sim \max(\Gamma, \Delta\omega)$, we obtained the spectrum $\Phi_F(\omega)$
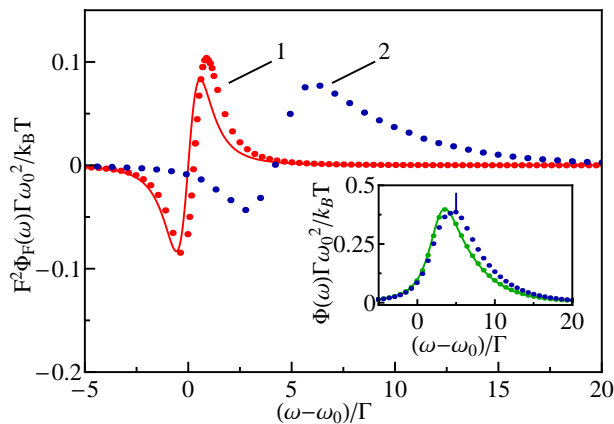
FIG. 6. The driving-induced part of the spectrum of a non-linear oscillator for small detuning of the driving frequency. The solid curve (red) shows the analytical results for $\Phi_F(\omega)$ for small $\Delta\omega/\Gamma$ for the same parameters as the dotted curve 1. The dots show the results of simulations. The scaled values of the nonlinearity parameter, the detuning, and the driving strength on the curves 1 and 2 are, respectively, $\alpha \equiv \Delta\omega/\Gamma = 0.05$, and 1.25, $\delta\omega_F/\Gamma = 0.5$ and 5, and $\beta \equiv 3\gamma F^2/32\omega_0^3(\delta\omega_F)^3 = 0.64$ and 0.01. The inset shows the full spectrum for the parameters of curve 2 (blue dots, simulations); the spectrum without driving for the same $\Delta\omega/\Gamma$ is shown by the solid line (analytical) and (green) dots on top of this line, which are obtained by simulations.

by running numerical simulations. These results are presented in Fig. 6. They show that the general trend seen in Fig. 5 that $\Phi_F(\omega)$ changes signs and is asymmetric for a nonlinear oscillator persists in this case as well.

IX. CONCLUSIONS

In terms of experimental studies of mesoscopic vibrational systems, the major result of this paper is the suggestion of a way to single out and characterize the dispersive (nonresonant) coupling between vibrational modes. The proposed method allows revealing dispersive coupling even where there is no access to the mode coupled to the studied one. We have shown that dispersive coupling leads to a specific, generally double-peak extra structure in the power spectrum of a mode when this mode is driven close to resonance. The dispersive-coupling induced part of the power spectrum is quadratic in the driving field amplitude. It varies significantly with the detuning of the driving frequency from the mode eigenfrequency.

The "tune off to read off" approach, which relies on changing the driving frequency, allows one to study separately two effects. One is the dispersive-coupling induced broadening of the spectral peak of the linear response, which is of significant interest for mesoscopic modes.[1,7,8,16,17] The other is the decay of the "invisible" mode that is dispersively coupled to the studied mode. The double-peak structure of the driving-induced power

spectrum sensitively depends both on the strength of the dispersive coupling and the parameters of the invisible mode.

Another important feature of the driving-induced spectrum is the qualitative difference between the effects of nonlinear dispersive coupling to other modes and the internal nonlinearity of the studied mode. Both nonlinearities are known to broaden, in a somewhat similar way,[26] the linear response spectrum in the presence of thermal fluctuations. However, in the case of internal nonlinearity, the driving-induced part of the power spectrum changes sign as a function of frequency, i.e., it has peaks of the opposite signs and is similar (and is close, in a certain parameter range) to the derivative of the power spectrum without driving.

We have extended the results to the case of dispersive coupling to several modes. The contributions of different modes to the frequency fluctuations of the studied mode, and therefore to the random accumulation of its phase, are additive and mutually independent. Then the averaging over the phase accumulation can be done independently for each mode. The extension to the case of a few modes is therefore straightforward. New features emerge if there are many, but not too many modes. The cumulative effect of weak dispersive coupling to many modes may lead to an effectively strong coupling. As a result, the spectrum without driving becomes close to Gaussian in the central part, as was suggested in Ref. 1. The driving-induced part of the power spectrum displays a characteristic structure, which sensitively depends both on the parameters of the dispersive coupling and the dissipation parameters of the involved modes.

In terms of the theory, the paper describes a path-integral method that enables finding in an explicit form the spectrum of a driven oscillator in the presence of non-Gaussian fluctuations of its frequency, which result from dispersive coupling to other modes. The results apply for an arbitrary ratio between the relevant parameters of the system. These parameters are the magnitude (standard deviation) of the frequency fluctuations $\Delta\omega$, their reciprocal correlation time, which is given by the decay rate of the dispersively-coupled mode that causes the fluctuations, the decay rate of the driven mode itself, and the detuning of the driving frequency.

It is the presence of several parameters that makes it complicated to identify the broadening mechanisms from the linear response spectra. The results of the paper show the qualitative difference between the effects of these parameters on the power spectrum when the oscillator is driven. This enables their identification.

Generally, in mesoscopic vibrational systems, and in particular in nanomechanical systems, the internal (Duffing) and dispersive nonlinearities can be of the same order of magnitude. If the studied mode has a much higher frequency than the mode to which it is dispersively coupled, its fluctuations can be comparatively weaker making the effect of the dispersive coupling stronger. Also if there are several modes dispersively coupled to the

mode of interest, their cumulative effect can be stronger than the effect of the internal nonlinearity. This makes it even more important to be able to distinguish the effects, which the proposed approach allows.

The results immediately extend to the parameter range where the driven mode has high frequency and is in the quantum regime, $\hbar\omega_0 > k_B T$. This is because, as long as the mode itself is linear, its displacement is a superposition of the displacement without driving, which is affected by quantum fluctuations, and the classical driving-induced displacement. The effect of dispersive coupling to a classical mode ($\hbar\omega_d \ll k_B T$) on the driving-induced displacement is independent of $\hbar\omega_0/k_B T$. Dispersive coupling of a quantum mode to a classical mode is of particular interest for optomechanics, where the high-frequency optical cavity mode can be dispersively coupled to a low-frequency mechanical mode.[9,19] Driving the cavity mode leads in this case to a characteristic radiation described in this paper.

Appendix A: The transfer-matrix type construction

The central part of the calculation of the driving-induced power spectrum is the averaging over the frequency noise due to dispersive coupling. Equations (14) and (21) reduce this averaging to solving an ordinary differential equation (20) with the coefficient that varies with time stepwise. The solution can be simplified by taking advantage of this specific time dependence.

From Eq. (16), the interval (t_0, t) in Eq. (20) is separated into three regions $m = 1, 2, 3$ within which the time-dependent coefficient $k(t'') = \bar{k}_m$ is constant. The boundaries between the regions τ and τ' and the values of $\bar{k}_m$ are specified in Eq. (16). We enumerate the regions in the order of decreasing time, that is, the region $\tau < t'' < t$ corresponds to $m = 1$, etc. In each region

$$D(t''; k) = M_{11}(t'' - t_0; m)A_m + M_{12}(t'' - t_0; m)B_m. \tag{A1}$$

Here, M_{ij} are the matrix elements of the matrix

$$\hat{M}(t''; m) = \begin{pmatrix} \cosh a_m t'' & \sinh a_m t'' \\ a_m \sinh a_m t'' & a_m \cosh a_m t'' \end{pmatrix},$$
$$a_m \equiv a(\bar{k}_m) = \Gamma_d(1 - 4i\alpha_d \bar{k}_m)^{1/2} \tag{A2}$$

We note that, from Eq. (16), $a_1 = \Gamma_d(1 + 4i\alpha_d \mathrm{sgn}\gamma_d)^{1/2}$, whereas $a_2 = \Gamma_d$; a_3 is equal to either a_1 or a_1^* depending on whether $t' < t_1'$ or $t' > t_1'$ in the argument of the G-function in (21).

The values of A_1, B_1 in Eq. (A1) are determined by the conditions $D(t; k) = 1, \dot{D}(t; k) = -\Gamma_d$. The values of A_m, B_m for $m = 2, 3$ are found from the continuity of $D(t''; k), \dot{D}(t''; k)$ at the boundaries $t'' = \tau, \tau'$.

Function $G(t, t', t_1')$ in Eq. (21) is determined by $D(t_0; k) = A_3$ and $\dot{D}(t_0; k) = a_3 B_3$. From Eqs. (A1) and (A2) we have

$$\begin{pmatrix} A_3 \\ B_3 \end{pmatrix} = \hat{M}^{-1}(\tau' - t_0; 3)\hat{M}(\tau' - t_0; 2)\hat{M}^{-1}(\tau - t_0; 2)$$
$$\times \hat{M}(\tau - t_0; 1)\hat{M}^{-1}(t - t_0; 1)\begin{pmatrix} 1 \\ -\Gamma_d \end{pmatrix}, \tag{A3}$$

This simple relation combined with Eq. (21) give the integrand in the expression for the power spectrum $\Phi_F(\omega)$ in a simple form, which is convenient for numerical integration. The expression (A3) can be evaluated in the explicit form. The result is given in Sec. V C. It is advantageous when one looks for the asymptotic expressions for the spectrum $\Phi_F(\omega)$.

Appendix B: Alternative path-integral approach to averaging over frequency noise

Here we provide an alternative approach to evaluating function $G(t, t', t_1')$, which is defined by Eq. (15) and describes the outcome of averaging over the frequency noise. The method is related, albeit fairly remotely, to the method developed for calculating the power spectrum of a nonlinear oscillator in the absence of driving.[20,26] We start with writing the probability density functional of the Gaussian process $Q_d(t)$ on the whole time axes, $-\infty < t < \infty$, in terms of the correlation function $A(t_2, t_3) = \langle Q_d(t_2)Q_d(t_3)\rangle$ and its inverse $A^{-1}(t_2, t_3)$,

$$\mathcal{P}[Q_d(t)] = \exp\left[-\frac{1}{2}\int\int dt_1 dt_2 Q_d(t_1)A^{-1}(t_1, t_2)Q_d(t_2)\right],$$
$$\int dt_2 A^{-1}(t_1, t_2)A(t_2, t_3) = \delta(t_1 - t_3), \tag{B1}$$

cf. Ref. 36).

From Eq. (15), function G and its derivative $\partial G/\partial t$ can be written as

$$G(t, t', t_1') = \frac{\int \mathcal{D}[Q_d]\tilde{\mathcal{P}}[Q_d]}{\int \mathcal{D}[Q_d]\mathcal{P}[Q_d]},$$
$$\frac{\partial G}{\partial t} = -i\mathrm{sgn}(\gamma_d)\frac{\int \mathcal{D}[Q_d]Q_d^2(t)\tilde{\mathcal{P}}[Q_d]}{\int \mathcal{D}[Q_d]\mathcal{P}[Q_d]}, \tag{B2}$$

where functional $\tilde{\mathcal{P}}$ has the form

$$\tilde{\mathcal{P}}[Q_d] = \exp\left[-\frac{1}{2}\int\int dt_1 dt_2 Q_d(t_1)\tilde{A}^{-1}(t_1, t_2)Q_d(t_2)\right],$$
$$\tilde{A}^{-1}(t_1, t_2) = A^{-1}(t_1, t_2) - 2ik(t_2)\delta(t_1 - t_2). \tag{B3}$$

Here $k(t_2)$ is a stepwise function, which is equal to 0 or ± 1 in the time interval (t_0, t), where $t_0 \equiv \min(t', t_1')$ is

defined in Eq. (16). This definition has to be extended in the present formulation, $k(t_2) = 0$ for $t_2 > t$ and $t_2 < t_0$.

A key observation is that functional $\tilde{\mathcal{P}}[Q_d]$ is also Gaussian. One can introduce an operator $\tilde{A}(t, t_1)$ reciprocal to $\tilde{A}^{-1}$,

$$\int dt_1 \tilde{A}(t, t_1) \tilde{A}^{-1}(t_1, t_2) = \delta(t - t_2). \quad \text{(B4)}$$

In terms of this operator,

$$\tilde{A}(t, t) = \frac{\int \mathcal{D}[Q_d] Q_d^2(t) \tilde{\mathcal{P}}[Q_d]}{\int \mathcal{D}[Q_d] \tilde{\mathcal{P}}[Q_d]} \quad \text{(B5)}$$

where $\tilde{A}$ is related to $\tilde{A}^{-1}$ through

$$\int dt_1 \tilde{A}(t, t_1) \tilde{A}^{-1}(t_1, t_2) = \delta(t - t_2). \quad \text{(B6)}$$

Multiplying equation (B3) for $\tilde{A}^{-1}$ by $A(t_2, t_3)\tilde{A}(t_1, t)$ and integrating with respect to t_1, t_2, we obtain an integral equation for $\tilde{A}(t, t_3)$,

$$\tilde{A}(t, t_3) - 2i \int k(t_1) \tilde{A}(t, t_1) A(t_1, t_3) dt_1 = A(t, t_3). \quad \text{(B7)}$$

This equation can be reduced to a differential equation by differentiating twice with respect to t_3,

$$\frac{\partial^2 \tilde{A}(t, t_3)}{\partial t_3^2} - \Gamma_d^2[1 - 4i\alpha_d k(t_3)]\tilde{A}(t, t_3) = -2\alpha_d \Gamma_d^2 \delta(t_3 - t). \quad \text{(B8)}$$

Interestingly, Eq. (B8) has the same structure as the differential equation for the "time-dependent" determinant found in the other method, see Eq. (20). Thus it can be solved in a similar fashion as in Appendix (A). The boundary conditions are $\tilde{A}(t, \pm\infty) = 0$. It follows from the decay of correlations of $Q_d(t)$. At the values of t_3 where $k(t_3)$ changes stepwise, see Eq. (16), $\tilde{A}$ and $\partial\tilde{A}/\partial t_3$ remain continuous, except $t_3 = t$, where $\partial\tilde{A}/\partial t_3$ changes by $2\alpha_d \Gamma_d^2$, as seen from Eq. (B8).

We can now write Eq. (B3) for function $G(t, t', t_1')$, in terms of function $\tilde{A}$,

$$\partial_t G(t, t', t_1') = -i\,\mathrm{sgn}(\gamma_d)\tilde{A}(t, t)G. \quad \text{(B9)}$$

The boundary condition for this equation is $G(t, t, 0) = 1$. From the explicit expression for G we also have

$$\partial_{t'} G(t, t', t_1') = i\,\mathrm{sgn}(\gamma_d)\tilde{A}(t', t')G(t, t', t_1'),$$

$$\partial_{t_1'} G(t, t', t_1') = -i\,\mathrm{sgn}(\gamma_d)\tilde{A}(t_1', t_1')G(t, t', t_1'). \quad \text{(B10)}$$

The solution of these equations reads

$$G(t, t', t_1') = \exp\left\{-i\,\mathrm{sgn}(\gamma_d)\left[\int_{t'}^{t} \tilde{A}(t'', t'')dt'' - \int_{t_1'}^{0} \tilde{A}(t'', t'')dt''\right]\right\}. \quad \text{(B11)}$$

We have checked that the expression for function G that follows from Eqs. (B8) and (B11) coincides with the result obtained in the main text.

Appendix C: Driving-induced spectrum for an effectively strong dispersive coupling to a large number of modes

Calculation of the driving-induced power spectrum involves a triple integral over time, as seen from Eq. (13). It is convenient to evaluate the integrals over t', t_1' separately in three regions, $A1$, $A2$, and $A3$. Region $A1$ corresponds to $-\infty < t' \le t_1', -\infty < t_1' \le 0$; then in Eq. (33) $\tau_1 = t, \tau_2 = -t_1', \tau_3 = t_1' - t'$. Region $A2$ corresponds to $-\infty < t_1' \le t', -\infty < t' \le 0$; then in Eq. (33) $\tau_1 = t, \tau_2 = -t', \tau_3 = t' - t_1'$. Region $A3$ corresponds to $0 < t' \le t, -\infty < t_1' \le 0$; then in Eq. (33) $\tau_1 = t - t', \tau_2 = t', \tau_3 = -t_1'$. Expanding the exponentials in $G^2(t, t', t_1')$ as described in Sec. VII A and integrating G^2 with weight $\exp[-(\Gamma - i\delta\omega_F)(t - t') + (\Gamma + i\delta\omega_F)t_1']$ [see Eq. (13)], we obtain the contributions of the regions $A1$ and $A2$ in the form

$$\Phi_F^{(A1)}(\omega) \approx -\frac{1}{2}\mathrm{Re}\sum_{n=0}^{\infty}\mathcal{K}_n \frac{\partial^n\chi(\omega)}{\partial\omega^n}\frac{\partial^n\chi(\omega_F)}{\partial\omega_F^n},$$

$$\mathcal{K}_{n>0} = \frac{4^n}{n!}\sum_{\varkappa_1, \ldots, \varkappa_n}\alpha_{\varkappa_1}^2 \ldots \alpha_{\varkappa_n}^2 \Gamma_{\varkappa_1}^2 \ldots \Gamma_{\varkappa_n}^2 [2\Gamma + 2\sum_{i=1}^{n}\Gamma_{\varkappa_i}]^{-1}$$

$$\Phi_F^{(A2)}(\omega) \approx \frac{1}{2}\mathrm{Re}\sum_{n=0}^{\infty}\mathcal{K}_n \frac{\partial^n\chi(\omega)}{\partial\omega^n}\frac{\partial^n\chi^*(\omega_F)}{\partial\omega_F^n}. \quad \text{(C1)}$$

In this equation $\mathcal{K}_0 = 1/2\Gamma$. The susceptibility

$$\chi(\omega) = (i/2\omega_0)\int_0^{\infty}dt\, e^{i(\omega - \tilde{\omega}_0)t - \Gamma t - \sigma^2 t^2/2} \quad \text{(C2)}$$

can be easily expressed in terms of the error function; $\tilde{\omega}_0$ and σ^2 are given by Eqs. (31) and (32).

In the region $A3$ it is convenient first to change from integration over t' to integration over $\tilde{t}' = t - t'$. To find the spectrum Φ_F, it is convenient to integrate G^2 with the appropriate weight first over t and then over $\tilde{t}'$. One should take into account that $\tilde{t}' \lesssim 1/\sigma \ll 1/\Gamma_\varkappa$, but the range of the values of t that contribute to the integral is not limited to $\lesssim 1/\sigma$. The result of integration reads

$$\Phi_F^{(A3)}(\omega) \approx -\mathrm{Im}[\chi(\omega)\chi^*(\omega_F)]/[2(\omega - \omega_F)]$$

$$+ \frac{1}{2}\mathrm{Re}\sum_{n=1}^{\infty}\mathcal{K}_n' \frac{\partial^n\chi(\omega)}{\partial\omega^n}\frac{\partial^n\chi^*(\omega_F)}{\partial\omega_F^n}. \quad \text{(C3)}$$

Here, the coefficients $\mathcal{K}_n'$ are given by the expression (C1) for $\mathcal{K}_n$ in which 2Γ is replaced by $-i(\omega - \omega_F)$. We note that $\Phi_F^{(A3)}$ is not singular at $\omega = \omega_F$, since $\mathrm{Im}\,|\chi(\omega_F)|^2 = 0$ and $\chi(\omega)$ is a smooth function of frequency; the corresponding term is important primarily where either ω or ω_F are on the tail of the spectral peak $\Phi_0(\omega)$.

The series over n in Eqs. (C1) and (C3) generally converges slowly if the decay rates of the $\varkappa$ modes $\Gamma_\varkappa \lesssim \Gamma$. For large n, in Eq. (C3) the derivative $\partial^n\chi(\omega)/\partial\omega^n$ should be calculated with the decay rate Γ replaced with

$\Gamma + 2\sum_{i=1}^{n} \Gamma_{\varkappa_i}$ in Eq. (C2). The summation over the modes $\varkappa_i$ in the coefficients $\mathcal{K}'_n$ should now be extended to include the modified $\chi(\omega)$, which now itself depends on $\varkappa_i$. We note that $\chi^*(\omega_F)$ in Eq. (C3) should still be calculated using Eq. (C2).

The overall driving-induced term in the power spectrum $\Phi_F(\omega) = \Phi_F^{(A1)}(\omega) + \Phi_F^{(A2)}(\omega) + \Phi_F^{(A3)}(\omega)$ has peaks and, generally, more complicated features near both the oscillator eigenfrequency and the driving frequency.

[1] A. W. Barnard, V. Sazonova, A. M. van der Zande, and P. L. McEuen, PNAS **109**, 19093 (2012).

[2] A. Eichler, M. del Álamo Ruiz, J. A. Plaza, and A. Bachtold, Phys. Rev. Lett. **109**, 025503 (2012).

[3] H. J. R. Westra, M. Poot, H. S. J. van der Zant, and W. J. Venstra, Phys. Rev. Lett. **105**, 117205 (2010).

[4] A. Castellanos-Gomez, H. B. Meerwaldt, W. J. Venstra, H. S. J. van der Zant, and G. A. Steele, Phys. Rev. B **86**, 041402 (2012).

[5] I. Mahboob, K. Nishiguchi, H. Okamoto, and H. Yamaguchi, Nat. Phys. **8**, 387 (2012).

[6] I. Mahboob, K. Nishiguchi, A. Fujiwara, and H. Yamaguchi, Phys. Rev. Lett. **110**, 127202 (2013).

[7] M. H. Matheny, L. G. Villanueva, R. B. Karabalin, J. E. Sader, and M. L. Roukes, Nano Lett. **13**, 1622 (2013).

[8] T. F. Miao, S. Yeom, P. Wang, B. Standley, and M. Bockrath, Nano Lett. **14**, 2982 (2014).

[9] J. C. Sankey, C. Yang, B. M. Zwickl, A. M. Jayich, and J. G. E. Harris, Nat. Phys. **6**, 707 (2010).

[10] T. P. Purdy, D. W. C. Brooks, T. Botter, N. Brahms, Z.-Y. Ma, and D. M. Stamper-Kurn, Phys. Rev. Lett. **105**, 133602 (2010).

[11] M. Aspelmeyer, T. J. Kippenberg, and F. Marquardt, eds., *Cavity Optomechanics* (Springer, Heidelberg, 2014).

[12] V. Singh, S. J. Bosman, B. H. Schneider, Y. M. Blanter, A. Castellanos-Gomez, and G. A. Steele, Nat Nano **9**, 820 (2014).

[13] P. Weber, J. Güttinger, I. Tsioutsios, D. E. Chang, and A. Bachtold, Nano Lett. **14**, 2854 (2014).

[14] T. K. Paraïso, M. Kalaee, L. Zang, H. Pfeifer, F. Marquardt, and O. Painter, ArXiv e-prints (2015), arXiv:1505.07291.

[15] E. T. Holland, B. Vlastakis, R. W. Heeres, M. J. Reagor, U. Vool, Z. Leghtas, L. Frunzio, G. Kirchmair, M. H. Devoret, M. Mirrahimi, and R. J. Schoelkopf, ArXiv e-prints (2015), arXiv:1504.03382.

[16] W. J. Venstra, R. van Leeuwen, and H. S. J. van der Zant, Appl. Phys. Lett. **101**, 243111 (2012).

[17] A. Vinante, Phys. Rev. B **90**, 024308 (2014).

[18] D. H. Santamore, A. C. Doherty, and M. C. Cross, Phys. Rev. B **70**, 144301 (2004).

[19] M. Ludwig, A. H. Safavi-Naeini, O. Painter, and F. Marquardt, Phys. Rev. Lett. **109**, 063601 (2012).

[20] M. I. Dykman and M. A. Krivoglaz, in *Sov. Phys. Reviews*, Vol. 5, edited by I. M. Khalatnikov (Harwood Academic, New York, 1984) pp. 265–441, http://www.pa.msu.edu/dykman/pub06/DKreview84.pdf.

[21] M. Sansa, E. Sage, E. C. Bullard, M. Gely, T. Alava, E. Colinet, A. K. Naik, G. L. Villanueva, L. Duraffourg, M. L. Roukes, G. Jourdan, and S. Hentz, ArXiv e-prints (2015), arXiv:1506.08135.

[22] Y. Zhang, J. Moser, J. Güttinger, A. Bachtold, and M. I. Dykman, Phys. Rev. Lett. **113**, 255502 (2014).

[23] H. A. Lorentz, *The theory of electrons and its applications to the phenomena of light and radiant heat* (Teubner, B. G., Leipzig, 1916).

[24] A. Einstein and L. Hopf, Ann.d. Phys. **33**, 1105 (1910).

[25] W. Heitler, *The Quantum Theory of Radiation, 3rd ed.* (Dover Publications, Inc., New York, 2010).

[26] M. I. Dykman and M. A. Krivoglaz, Phys. Stat. Sol. B **48**, 497 (1971).

[27] P. W. Anderson, J. Phys. Soc. Japan **9**, 316 (1954).

[28] R. Kubo, J. Phys. Soc. Japan **9**, 935 (1954).

[29] M. I. Dykman and M. A. Krivoglaz, Fiz. Tverd. Tela **29**, 368 (1987).

[30] A. A. Clerk and D. W. Utami, Phys. Rev. A **75**, 042302 (2007).

[31] D. I. Schuster, A. A. Houck, J. A. Schreier, A. Wallraff, J. M. Gambetta, A. Blais, L. Frunzio, J. Majer, B. Johnson, M. H. Devoret, S. M. Girvin, and R. J. Schoelkopf, Nature **445**, 515 (2007).

[32] I. R. Senitzky, Phys. Rev. **119**, 670 (1960).

[33] J. Schwinger, J. Math. Phys. **2**, 407 (1961).

[34] W. H. Louisell, *Quantum Statistical Properties of Radiation* (Wiley-VCH, Berlin, 1990).

[35] I. M. Gelfand and A. M. Yaglom, J. Math. Phys. **1**, 48 (1960).

[36] R. P. Feynman and A. R. Hibbs, *Quantum Mechanics and Path Integrals* (McGraw-Hill, New-York, 1965).

[37] R. Phythian, J. Phys. A **10**, 777 (1977).

[38] R. Mannella, Int. J. Mod. Phys. C **13**, 1177 (2002).

[39] M. A. Ivanov, L. B. Kvashnina, and M. A. Krivoglaz, Sov. Phys. Solid State **7**, 1652 (1965).

[40] R. J. Elliott, W. Hayes, G. D. Jones, H. F. MacDonald, and C. T. Sennett, Proc. Roy. Soc. London **A289**, 1 (1965).

[41] M. I. Dykman, ed., *Fluctuating Nonlinear Oscillators: from Nanomechanics to Quantum Superconducting Circuits* (OUP, Oxford, 2012).

[42] Y. Zhang, Y. Tadokoro, and M. I. Dykman, NJP **16**, 113064 (2014).

[43] L. D. Landau and E. M. Lifshitz, *Mechanics*, 3rd ed. (Elsevier, Amsterdam, 2004).

[44] M. I. Dykman and M. A. Krivoglaz, Zh. Eksp. Teor. Fiz. **77**, 60 (1979).

[45] P. D. Drummond and D. F. Walls, J. Phys. A **13**, 725 (1980).